

1           New insight on tide-dominated estuary and delta in the  
2           Eocene-Miocene Mrayt Group, North-Western Rif, Morocco

3  
4           Naima Hamoumi<sup>1</sup>, Choukri Chacrone<sup>2</sup> ✉, Silvia Spezzaferri<sup>3</sup>

5  
6           <sup>1</sup>Research group ODYSSEE, Department of Earth Sciences, Mohammed V University, Rabat, Morocco

7           <sup>2</sup>Centre régional des métiers de l'éducation et de la Formation (CRMEF) de Casablanca Hay Hassani, Maroc

8           <sup>3</sup>Université de Fribourg, Department of Geosciences, Earth Sciences, 1700 Fribourg, Switzerland

9  
10          Correspondance: ✉ Choukri Chacrone

11          choukrichacrone@gmail.com

12  
13  
14          This manuscript is a non-peer reviewed EarthArXiv preprint, and has been  
15          submitted for publication in Arabian Journal of Geosciences.

1 Abstract

2 The sedimentary deposits of Eocene-Miocene Mrayt Group, North-Western Rif, Morocco has been the subject of  
3 controversy by previous authors regarding their depositional environment. Detailed sedimentological study  
4 based on petrographic and sedimentary facies analysis, ichnofacies interpretation and paleocurrent  
5 measurements, leads to several results and new insights.

6 Petrographic study provided the first evidence of mixed siliciclastic and carbonate sediments and their  
7 nomenclature: silty micrites, micritic siltstones, micritic sandstones, sandy micrite, and allochemic sandstones,  
8 as well as the nature of the sources and its geological context.

9 Twenty two sedimentary facies that have never been described before are identified, and based on their  
10 succession and association a new interpretation of depositional processes and depositional systems are proposed.  
11 The paleoenvironments of the Mrayt Group are interpreted as littoral and shallow marine settings: tides-  
12 dominated estuary, tides-dominated delta systems and open coast tidal flat, under complex hydrodynamics  
13 strongly influenced by river discharge, tidal currents, waves and storms action.

14 Sedimentation occurred in “the Maghrebian basin” under the interplay of: i) tectonics related to the  
15 Cenozoic collision of the African and Eurasian continental plates, ii) Cenozoic alternation of warm climate and  
16 cooling due to the increasing influence of Antarctica glaciation, iii) sediments supplies induced by rejuvenation  
17 of sedimentary sources and iv) sea level fluctuation related to the advance and retreat of ice-sheet on Antarctica.

18

19 **Key words** Tide dominated delta, mixed siliciclastic/carbonate sediment, Mrayt Group, NW Rif, Morocco,  
20 Eocene –Miocene

21

22

23 Introduction

24 The alpine Rif belt has been studied since 1846 in the frame of several national and International programs. Most  
25 of these researches focused on tectonic, geochemistry, petrography, biostratigraphy and geophysics, while  
26 sedimentology was mostly neglected. Thus, the paleogeography and the geology of the region reported in  
27 geological maps of the NW Rif sections were interpreted without taking into account the sedimentary facies.

28 This has given origin, to the many controversies on the relationships between the tectono-paleogeographic units,  
29 their lithostratigraphy and the nature of the sediments. The paleogeography in this area is complex and mostly

1 unconstrained, therefore, sedimentological facies and depositional environmental analysis is important to  
2 reconstruct this.

3 Sedimentological studies conducted in the flysch domain of the NW Rif belt, in the framework of “The  
4 Linked Project Cross the Strait of Gibraltar between Africa and Europe” (Hamoumi 1995a; Hamoumi et al.  
5 1995; Ouldchelha et al. 1995; Salhi et al. 1995), has highly contributed to the knowledge of the depositional  
6 environments that prevailed over the Cretaceous-Miocene period and their allogenic and autogenic control.  
7 The Eocene-Miocene Mrayt Group, in the North Western Rif, Morocco was described for the first time by Suter  
8 and Fiechter (1966) and called “Flysch de Sidi Mrayt” by Suter (1986). It has been studied for its tectonics,  
9 lithostratigraphy, biostratigraphy and sedimentology (Suter and Fiechter 1966; Suter 1980; Suter 1986; Morley  
10 1992; Tejera de Leon 1993; Abdelkhaliki 1997; Raissouni et al. 2008). Although these studies have agreed on  
11 the lithostratigraphic characteristics of these sediments, there are, however, discrepancies concerning the  
12 environment in which they were deposited. Indeed, the deposits of this group have been interpreted as: 1)  
13 synorogenic turbidites organized in two sequences (Morley 1992): a lower sequence referred to a Type I deep  
14 sea fan system, and an upper sequence linked to a Type III deep sea fan system (sensu Mutti 1985); 2) reworked  
15 and redeposited slope sediments by bottom currents on an abyssal plain, capped by slides and mass flow deposits  
16 that accumulate at the end of slope in un-channelized areas (Tejera de Leon 1993); 3) a sedimentary prism  
17 adjacent to the outer edge of the platform subjected to storm waves action and passing to a Mutti type III deep  
18 sea fan system (Raissouni et al. 2008).

19 Detailed sedimentological study conducted for the first time in the Mrayt Group, allows bringing new  
20 results concerning: the nature of the sediments and their sources, the sedimentary facies, the depositional  
21 systems, the sedimentary processes and the allogenic control. The aims of this work are: 1) to highlights the  
22 mixed composition (siliciclastic/carbonate) of the Mrayt Group sediments and to introduce a more adequate  
23 nomenclature for these deposits; 2) to bring new findings, including the characterization of new sedimentary  
24 facies never described before and a new interpretation of the depositional processes and sedimentary  
25 environments corresponding to tide-dominated estuary, tide-dominated delta systems and open-coast tidal flat; 3)  
26 to document the evolution from tide-dominated estuary to tide-dominated delta and then to open-coast tidal flat  
27 and it's control during the Eocene–Miocene in the Rif alpine belt.

28 In addition to these new results this study is important for increasing our knowledge about ancient tide-  
29 dominated delta that is less investigated in comparison to the other deltaic systems (waves or river dominated)

1 and its responses to sea level changes and tectonics. Tide- dominated deltas are those where tide currents are the  
2 dominant process controlling sediment dispersal (Galloway 1975; Goodbread and Saito 2012, and references  
3 therein). Furthermore correct interpretation of Eocene–Miocene sedimentary sections of the North Western Rif is  
4 essential to understand the paleogeography and the geodynamic evolution of the Rif alpine belt which is a part of  
5 the peri Mediterranean alpine belt. It's also critical for regional economies as deltas may contain significant  
6 volumes of oil and gaz.

7

## 8 Geological setting

9

10 The Mrayt Group is a 1730 m-thick sedimentary unit crops out in the North Western Rif along the Atlantic  
11 littoral between the cities of Asilah and Larache in North Morocco (Fig.1). It belongs to the Prerif domain of the  
12 Rif belt (Suter and Fiechter 1966). The Rif belt represents the westernmost part of the Maghrebide belt that  
13 belongs to the western part of the alpine Mediterranean orogen and its connected to the Betic belt through the  
14 Gibraltar arc (Fig.1A). It corresponds to a syntectonic province characterized by the alpine folding related to the  
15 Tertiary collision between Alboran microplate, the Iberian plate and the African from the Oligocene to the Late  
16 Miocene (9-8 Ma) (Dewey et al. 1989; Srivastava et al. 1990; Leprêtre et al. 2018 and references therein).

17 The Rif belt (Fig.1B) is composed of three main structural units, from West to East: i) the “external Zone”  
18 that consists of three stacked units (in ascending order): the Prerif, the Mesorif and the Intrarif, ii) the flysch  
19 thrust sheets composed of several tectonic units as the Numidian flyschs, the Mauritanian flyschs and the  
20 Merinide flyschs and iii) the “internal Zone” considered as a part of the “Thetysian Alboran Terrane” (Durand-  
21 Delga et al. 1962; Andrieux 1971; Suter 1980).

22 The Mrayt Group (Fig.1B and Fig.1C) crops out in the North western “external Zone” of the Rif North of  
23 the Jebha-Chrafat accident and is overlapped to the East by the allochthonous Habt unit (Suter 1980 and 1986).  
24 It's deformed by a section of anticline and syncline folds trending S-N, and separated by overthrust faults (Tejera  
25 de Leon 1993). Stratigraphically, the Mrayt Group rests on Cretaceous marlstones and consists of four  
26 Formations (Tabl.1) from base to top: Lower pelitic” formation, Sandstone-pelitic formation, Upper sandstone-  
27 pelitic formation and Si Moussa Formation which rests unconformably on the underlying formation. These  
28 formations are ranging in age from the Lower Eocene to the Middle Miocene based on microfossils (Suter and  
29 Fiechter 1966; Suter 1980 and 1986; and Tejera de Leon 1993).

1

2 **Tabl. 1** Lithostratigraphy of the Mrayt Group formations (after Suter and Fiechter 1966; Suter 1980 and 1986; and  
3 Tejera de Leon 1993)

Formation		Thickness	Lithology	Age
Si Moussa Formation		500 m	Interbedded sandstones and marly pelites	Middle Miocene (Langhian)
Upper pelitic Formation		100 m	Interbedded sandstones and pelites	Upper Oligocene to Lower Miocene
Sandstone and pelitic Formation	Upper conglomeratic member	400 m	Interbedded sandstones, pelites and conglomerates	Early to Upper Oligocene
	Lower sandstones and pelitic member	600 m	Interbedded sandstones, pelites and microglomerates	
Lower pelitic Formation	Upper member	100 m	Interbedded sandstones and pelites	Lower Eocene
	Lower member	50 m	Interbedded microglomerats, sandstones and marlstones	

4

## 5 Methods

6

7 Five sections belonging to the Mrayt Group, totalizing 1730 m in thickness has been logged bed by bed (Fig.  
8 1C). They are named: MG1- Damina section, 80m thick (X= 6.06; Y= 35.42), MG2- Marabout section, 750m  
9 thick (X= 5.85; Y= 35.36), MG3- Sidi Mrayt beach section, 200m thick (X= 5.85; Y= 35.41), MG4- Merja  
10 section, 520m thick (X= 5.96; Y= 35.43), and MG5- Merja ravine section, 280m thick (X= 6.05; Y= 35.44). In  
11 each section, sedimentary facies have been described to reconstruct depositional environments. Sedimentary  
12 facies are identified on the basis of their petrofacies and lithofacies. The petrofacies is here defined in term of  
13 composition and texture introduced for rocks classification (Mansfield 1971; Dickinson and Rich 1972). The  
14 determination of the composition takes into account the detrital, authigenic and organic constituents and the  
15 texture includes the proportion of clay matrix and the shape, roundness, surface features, grain size and fabric of  
16 the components. The petrographic study of the Mrayt Group deposits based on the examination of 50 thin

1 sections under polarizing microscope, indicate that the investigated sediments are composed of mixtures of  
2 siliciclastic sediments (sand and mud) and carbonate sediments (allochems and matrix). Therefore it was  
3 necessary to apply the classification of Mount (1985) in order to establish the precise nomenclature for the  
4 petrofacies. This classification defined eight general classes of mixed sediments. The name of the class is based  
5 on both dominant grain type and the most abundant antithetic components.

6 The lithofacies reconstruction is based on centimeter-scale description of outcrops. The lithofacies is here  
7 characterized by the lithology, color, thickness and geometry of the strata, the nature of their bounding surfaces  
8 together with associated sedimentary structures. The sedimentary facies identified were clustered into  
9 sedimentary facies association (Reading 1986) according to the following criteria: their environmental  
10 significance, their genetic relationship and their situation in relation to each other according to Collinson (1969)  
11 and Reading (1986). The paleocurrent measurements were performed on 48 flute casts in the five studied  
12 outcrops and the dip of longest axis of the clasts in the three conglomerate levels (Facies F17).

13

## 14 Sedimentary facies analysis

15

### 16 The Petrofacies

17

18 The Petrographical analysis show that the Mrayt Group deposits consist of mixed siliciclastic / carbonate  
19 sediments, composed of: siliciclastic and carbonate grains, matrix and cement (Fig. 2). The siliciclastic minerals  
20 consists of: 1) moderately sorted, angular, sub-rounded or rounded detrital quartz grains, that may be  
21 monocrystalline with undulating extinction or polycrystalline (polygonised quartz, slightly sutured grains and  
22 chert) and sometimes with a secondary quartz overgrowths; 2) sub-rounded to sub-angular, < 0.125 mm in size  
23 feldspar grains (microcline, plagioclase and orthoses) which are affected by alteration to various degrees ; 3)  
24 sub-rounded to angular, > 2 µm in size lithic clasts of sedimentary, volcanic or metamorphic origin,; 4) altered  
25 micas (muscovite, biotite and chlorite); 5) glauconitic grains; 6) heavy minerals (rounded zircons, green  
26 tourmaline) and 7) opaque minerals including iron oxides. Carbonate components consist of: calcite lithoclasts  
27 which may include benthic and planktonic foraminifera including e.g., Orbitolina and sometimes micritized  
28 Calpionella, skeletal fragments of: gastropods, bivalves, echinoderms, bryozoans and algae and sometimes

1 rhombohedral crystals of dolomite. The bonding phase is composed of carbonate cement (microsparite and  
2 sparite), ferruginous and siliceous cements, and sometimes by a clay matrix.  
3 Five petrofacies were identified (Fig. 2, photos A, B, C and D) according to Mount (1985) Classification:  
4 siltymicrites, micritic siltstones, micritic sandstones, sandy micrites, and allochemic sandstones. They are very  
5 similar to those observed within the Eocene to Miocene sedimentary series outcropping in the North Western Rif  
6 (Hamoumi 1995b; Hamoumi et al. 1995; Ouldchalha et al. 1995; Salhi et al. 1995). Their compositional mixing  
7 indicate contemporaneous accumulation and sediment supply from both intra-basinal and extra-basinal sources  
8 under the control of allocyclic (e.g. sea level, tectonics, climate) and/or autocyclic (depositional processes)  
9 factors. The presence in the siliciclastic fraction of undulatory monocrystalline quartz with sometimes secondary  
10 quartz overgrowths, polycrystalline quartz grains, volcanic and metamorphic rock fragments and micas  
11 (muscovite, biotite and chlorite) and the roundness of heavy minerals suggest a provenance from sedimentary,  
12 volcanic and high rank metamorphic sources. The existence of calcite lithoclasts which may include benthic and  
13 planktonic foraminifera including e.g., Orbitolina and sometimes micritized Calpionella, indicate extrabasinal  
14 carbonate sources including a source of Cretaceous age. The poor sediment sorting, as well as the presence of  
15 rock fragments, feldspar and biotite is in favor of rapid erosion from a young and high relief continental source  
16 and a short transport and rapid deposition. Alteration affecting feldspar and micas as well as small size and lower  
17 frequency of feldspar suggest a hydrolyzing (humid to semi-humid) climate. The intra-basinal source provides  
18 the shell fragments which results from reworking of in situ exoskeletons and glauconitic peloids. Algae and  
19 rhombohedral crystals of dolomite, suggest nearshore to shallow marine depositional setting. Glauconite is  
20 authigenic and forms in shallow marine environment under reducing to slightly oxidizing conditions (Pettijhon et  
21 al. 1973, Odin 1985).

22 . The micritization which affects Calpionella is probably is inherited from the source. It can neither be generated  
23 by organisms such bacteria or algae, nor be linked to burial compaction, because it does not affect all  
24 microfossils. .

25

## 26 The Sedimentary Facies

27

28 Sedimentological field studies combined with petrofacies analysis have resulted in the recognition for the first  
29 time of twenty two sedimentary facies, in the five studied outcrops of the Mrayt Group (Fig. 3, 4, 5, 6, 7 and 12).

1 Facies F1 (Fig. 3A and Fig. 6), is observed in the lower Pelitic Formation of Early to Middle Eocene age  
2 (Fig. 3). It consists of alternating centimetric to decimetric micritic siltstone bed and decimetric bioturbated marl  
3 interbed. The bed has an undulated; erosive lower base and generally contain five intervals (from base to top): 1)  
4 an interval (a) limited to its top by a reactivation surface and made up of successive couplets of thick (1-5cm)  
5 and thin (0,5-1cm) planar parallel micritic siltstone laminae limited each one to its upper surface by very thin  
6 mud layers (mm-scale) or mud drapes, 2) an interval (b) composed of ripple- cross- stratified micritic siltstone  
7 and mud layer slightly following the concavity and convexity of the underlying rippled surface, 3) an interval (c)  
8 with alternating planar parallel laminae of silty micrite and mud drapes, 4) an interval (d) composed of ripple-  
9 cross-laminated micritic siltstone which display symmetrical and asymmetrical ripples in which small lenses of  
10 mud are preserved in the trough of the ripple and 5) an interval (e) composed of micritic siltstone with ripples  
11 that vary in size and shape in the same layer. The top of bed shows centimetric to decimetric-scale desiccation  
12 cracks.

13 Facies F2 (Fig. 3B and Fig. 6), occurs in the lower Pelitic Formation of Early to Middle Eocene age (Fig.  
14 3). It consists of alternating centimetric to decimetric micritic siltstone bed and decimetric bioturbated marl  
15 interbed. The bed is erosively based and display three intervals (from base to top): 1) an interval (a) composed of  
16 ripple-cross- laminated micritic siltstone which display symmetrical and asymmetrical ripples in which small  
17 lenses of mud are preserved in the trough of the ripples, 2) an interval (b) composed of ripple-cross -stratified  
18 micritic siltstone and mud layers, slightly following the concavity and convexity of the underlying rippled  
19 surface, and 3) an interval (c) composed of rippled micritic siltstone lenses on a muddy layer. The top of bed  
20 shows Zoophycos trace fossil, Psilonichus Y-shaped burrows and centimetric to decimetric-scale desiccation  
21 cracks.

22 Facies F3 (Fig. 3C and Fig. 6), is identified in the lower Pelitic Formation of Early to Middle Eocene age  
23 and the upper part of the Sandstone and pelitic Formation of Upper Oligocene age (Fig. 3). It consists of  
24 lenticular, cm-thick sandy micrite layer, intercalated with metric pelitic level. The sandy micrite bed is erosively  
25 based and is composed of two intervals. The lower interval (a) is slightly deformed, without visible bedding and  
26 the upper interval (b) is characterized by asymmetrical ripples which may display two types of internal  
27 structures: 1) offshooting and draping laminations expressed by forest laminae which ascend and overlap the  
28 flank of the adjoining ripple, 2) composite internal structure made up of an assemblage of differently structured,



1 generally bidirectional lenses. The top of this interval contain straight-crested ripples and sometimes contains  
2 Zoophycos trace fossil, Psilonichus Y-shaped burrows and centimetric to decimetric-scale desiccation cracks.

3 Facies F4 (Fig. 3D and Fig. 6), occurs in the lower Pelitic Formation of Early to Middle Eocene age and the  
4 upper part of the Sandstone and pelitic Formation of Upper Oligocene age (Fig. 3). It consists of centimeter to  
5 decimetric lenticular sandy micrite bed intercalated with metric pelitic level. The bed has an erosively undulating  
6 base and an erosive top. It's composed of two intervals: the basal interval (a) comprises sets of parallel plane  
7 laminae, separated by reactivation surfaces. The upper interval (b) consists of tangential cross laminated cm-  
8 bundles separated by erosional surface and mud drape. The top of this interval exhibits centimetric to decimetric  
9 desiccation cracks.

10 Facies F5 (Fig. 3E and Fig. 6), is identified in the lower Pelitic Formation of Early to Middle Eocene age  
11 (Fig. 3). It consists of interbedded centimeter to decimetric silty micrite bed and decimetric bioturbated pelitic  
12 layer. The silty micrite bed has an erosive undulating base and its generally composed of 3 intervals: 1) a lower  
13 interval (a) exhibiting mud pebbles and asymmetric ripples characterized by a planar base and planar cross-  
14 lamination, 2) a structureless intermediate interval (b), and 3) an upper interval (c), characterized by parallel  
15 undulated laminations, pinching and swelling laterally and passing to incipient lenses. The top of the upper  
16 interval is characterized by linguoid ripples and may shows centimetric to decimetric desiccation cracks.

17 Facies F6 (Fig. 3F and Fig. 6) occurs in the lower Pelitic Formation of Early to Middle Eocene age (Fig. 3).  
18 It consists of alternating centimeter to decimetric silty micrite bed and decimetric bioturbated pelitic interbed. The  
19 bed is erosively based and comprises four intervals. The first interval (a) displays stacked sequences separated  
20 from each other by mud drapes, each sequence is composed of a set of thick laminae, which thin progressively  
21 from the bottom to the top. The second interval (b) is characterized by asymmetrical ripples displaying  
22 offshooting and draping laminations expressed by foreset laminae which ascend and overlap the flank of the  
23 adjoining ripple. The third interval is similar to the first one and the fourth interval is similar to the second one.  
24 The top of the bed exhibits straight-crested ripples.

25 Facies F7 (Fig. 3G and Fig. 6), is documented in the lower Pelitic Formation of Early to Middle Eocene age  
26 (Fig. 3). It consists of alternating centimeter to decimeter-thick micritic siltstone bed containing thin mud layers  
27 or mud drapes and decimetric bioturbated pelitic interbed. The bed has undulating erosive base and it's  
28 composed of 2 intervals. The lower interval (a) consists of stacked microsequences separated from each other by  
29 a reactivation surface. Each microsequence display successive couplets composed of thick (1-5cm) and thin (0,

1 5-1cm) planar parallel micritic siltstone laminae limited each one to its upper surface by very thin mud layers  
2 (mm-scale). The individual couplet thickness thin and thicken progressively from the bottom to the top of the  
3 microsequence. The upper interval (b) display sigmoid-shaped sets separated by reactivation surface or mud  
4 drape and made up of successive couplets composed of thick (1-5cm) and thin (0,5-1cm) sigmoidal oblique  
5 micritic siltstone laminae limited each one to its upper surface by very thin mud layers (mm-scale). The upper  
6 surface of this interval contains centimetric to decimetric-scale desiccation cracks.

7 Facies F8 (Fig. 4A and Fig. 6), is identified the lower Sandstone and pelitic Formation of Lower to Upper  
8 Oligocene age (Fig. 3). It corresponds to an alternation of centimetric silty micrite bed and metric pelitic  
9 interbed. The bed display planar parallel laminations or tabular cross-laminations that may be disturbed by  
10 convolute bedding. Its basal bounding surface is erosive and highly bioturbated, it sometimes show Paleodyction  
11 and Cruziana trace fossils.

12 Facies F9 (Fig. 4B and Fig. 6), is documented in the lower Sandstone and pelitic Formation of Lower to  
13 Upper Oligocene age (Fig. 3). It consists of alternating cm- to dm-thick sandy micrite bed and bioturbated pelitic  
14 dm-thick interbed. The bed is lenticular with tangential cross laminations and an erosive base exhibiting  
15 Paleodyction and Cruziana trace fossils, grooves casts, prod casts and bounce casts. The upper surface of the bed  
16 contains centimeter to decimetric desiccation cracks.

17 Facies F10 (Fig. 4C and Fig. 6), occurs in the lower Sandstone and pelitic Formation of Lower to Upper  
18 Oligocene age (Fig. 3). It consists of alternating decimetric pelitic interbed and centimetric to decimetric sandy  
19 micrite bed composed of 4 intervals (a, b, c and d from base to top), separated by erosional surface and mud  
20 drape. The first interval (a) exhibits an erosive base with grooves casts, prod casts, flute casts and Ophiomorpha  
21 burrows, and stacked microsequences separated from each other by a mud drapes. Each microsequence display  
22 successive couplets of thick (1-5cm) and thin (0, 5-1cm) planar parallel micritic siltstone laminae limited each  
23 one to its upper surface by very thin mud layers (mm-scale). The individual couplet thickness thin progressively  
24 from the bottom to the top of the microsequence. The second interval (b) is cross laminated characterized by  
25 asymmetrical ripples displaying various internal structures: 1) offshooting and draping laminations expressed by  
26 inclined foreset laminations passing the trough and ascending onto the flank of the adjacent ripple, 2) composite  
27 internal structure, made up of an assemblage of differently structured, generally multidirectional lenses, 3)  
28 swollen lens-like sets, and 4 ) undulating parallel laminations passing into cross laminations, The third interval  
29 (c) shows an undulating highly erosive lower bounding surface and it is fully disturbed by flame and convolute

1 structures. The fourth interval is similar to the first one, and display in its upper surface symmetrical ripples and  
2 mud pebbles.

3 Facies F11 (Fig. 4D and Fig. 6), is observed in the lower Sandstone and pelitic Formation of Lower to  
4 Upper Oligocene age (Fig. 3). It is composed of alternating decimetric lenticular allochemic sandstone bed, and  
5 decimetric pelitic interbed. The bed is erosively based with grooves casts, prod casts, bounce casts and flute casts  
6 may display convolute bedding, and it contains 3 intervals separated by reactivation surfaces. The lower interval  
7 (a) shows interbedded rippled sandy layers and continuous mud drapes overlapping the ripple troughs and crests.  
8 The intermediate interval (b) is a laminated sandy bed displaying sigmoidal cross laminations, successive foreset  
9 laminations directed in opposite directions in superimposed layers and reactivation surfaces. The upper interval  
10 (c) exhibits stacked microsequences separated from each other by mud drape. Each microsequence display  
11 successive couplets composed of thick (1-5cm) and thin (0, 5-1cm) planar parallel micritic siltstone laminae  
12 limited each one to its upper surface by very thin mud layers (mm-scale). The individual couplet thicknesses  
13 thicken progressively from the bottom to the top of the microsequence). The upper surface of this interval is  
14 erosive and may shows decimetric-scale desiccation cracks and mud pebbles.

15 Facies F12 (Fig. 4E and Fig. 6), occur in the lower Sandstone and pelitic Formation of Lower to Upper  
16 Oligocene age (Fig. 3). It consists of alternating centimeter to decimetric silty micrite bed containing thin mud  
17 layers or mud drapes and decimetric bioturbated pelitic interbed. The bed is erosively based with groove and flute  
18 casts, and comprises four intervals (a, b, c and d from base to top), separated by erosional surface and/or mud  
19 drape. The first interval (a) is composed of asymmetrical ripples characterized by lateral variation in size and  
20 shape in the same layer and irregular, undulating lower bounding surface, which may be disturbed by convolute  
21 bedding. The second interval (b) is made up of stacked microsequences separated from each other by a  
22 reactivation surface. Each microsequence display successive couplets composed of thick (1-5cm) and thin (0, 5-  
23 1cm) planar parallel micritic siltstone laminae, limited each one to its upper surface by very thin mud layers  
24 (mm-scale). The individual couplet thickness thin progressively from the bottom to the top of the microsequence.  
25 The third interval (c) is characterized by: 1) asymmetrical ripples displaying offshooting and draping laminations  
26 expressed by foreset laminae which ascend and overlap the flank of the adjoining ripple and 2) ripples displaying  
27 unidirectional cross lamina concordant with the lee side and laying on the same planar base. The fourth (d)  
28 interval exhibits tangential cross laminated cm-bundles, separated by erosional surfaces and mud drapes.

1 Facies F13 (Fig. 4F and 4G, and Fig. 6), occurs in the lower Sandstone and pelitic Formation of Lower to  
2 Upper Oligocene age (Fig. 3). It consists of alternating decimetric muddy layer and amalgamated decimetric,  
3 lenticular coarse-micritic sandstone bed. The bed has an erosively undulating base and an erosive top exhibiting  
4 metric scale wavelength hummocks, centimetric to decimetric desiccation cracks and soft pebbles. Its internal  
5 structure shows hummocky cross stratification expressed by successive lamina sets separated by low angle  
6 truncations surface and composed of parallel low-angle curved lamina which dome upward (hummocks) passing  
7 laterally into laminae that are concave upward (swaley).

8 Facies F14 (Fig. 4H and Fig. 6), is observed in the lower Sandstone and pelitic Formation of Lower to  
9 Upper Oligocene age (Fig. 3). It consists of interbedded, centimeter -to -decimeter -scale microconglomeratic  
10 bed with rich in organic matter and strongly bioturbated plurimetric pelitic layer. The bed has a lenticular shape  
11 and an erosive base with flute casts. It's made up of a fining upward microconglomerate containing rock clasts  
12 and shell fragments.

13 Facies F15 (Fig. 4I and Fig. 6), occur in the lower Sandstone and pelitic Formation of Lower to Upper  
14 Oligocene age (Fig. 3). It consists of alternation of decimetric pelitic layer and decimetric sequence of coarse-  
15 grained sediments. The sequence has an erosive base exhibiting flute casts and it is composed of 6 intervals  
16 (from base to top): 1) a lenticular metric fining upward microconglomerate containing rock clasts and shell  
17 fragments (a); 2) a massive allochemic sandstones with dish pillar structures and convolutes bedding (b); 3)  
18 ripple- cross-laminated micritic siltstone displaying unidirectional cross lamina concordant with the stoss side  
19 (c); 4) couplets of thick (1-5cm) and thin (0,5-1cm) planar parallel micritic siltstone laminae limited each one to  
20 its upper surface by very thin mud layers (mm-scale) separated sometime by reactivation surface (d); 5) micritic  
21 siltstone interval bounded by reactivation surfaces and exhibiting sigmoidal cross laminated bundle (e) and 6)  
22 micritic siltstone bed with asymmetrical ripples in which small lenses of mud are preserved in the trough of the  
23 ripple (f). The top of the sequence shows mud pebbles and Ophiomorpha and Skolithos burrows.

24 Facies F16 (Fig. 4J and Fig. 6), is documented in the lower Sandstone and pelitic Formation of Lower to  
25 Upper Oligocene age (Fig. 3). It consists of an alternation of decimetric pelitic layer and decimetric sequence of  
26 coarse-grained sediments. The sequence has an erosive base exhibiting flute casts and it's made up of 3 intervals.  
27 The lower interval (a) is a lenticular fining upward microconglomerate with rock clasts and shell fragments,  
28 displaying tangential cross-stratification, which pass upward into sandy micrite disturbed by convolutes bedding.  
29 The intermediate interval (b) is an allochemic sandstones composed of stacked microsequences separated from

1 each other by a mud drape. Each microsequence display successive couplets composed of thick (1-5cm) and thin  
2 (0, 5-1cm) planar parallel micritic siltstone laminae limited each one to its upper surface by very thin mud layers  
3 (mm-scale). The individual couplet thickness thin and thicken progressively from the bottom to the top of the  
4 microsequence. The upper interval (c) is an erosively based and cross-stratified silty micrite displaying: bundle  
5 of sigmoidal laminae separated by mud drapes and reactivation surfaces. The top of this sequence shows  
6 Zoophycos, and Ophiomorpha trace fossils.

7 Facies F17 occurs in the upper part of the lower Sandstone and pelitic Formation of Upper Oligocene age  
8 (Fig. 3); it can be divided into three subfacies: F17a, F17b and F17c Subfacies. F17a (Fig. 4K and Fig. 6) is a  
9 reddish brown lenticular coarse bed with sharp base ranging in thickness from 4 to 5 m. It consists of a matrix-  
10 supported conglomerate, structureless, ungraded and without any preferred clast imbrication/organization. The  
11 clasts consist of pelite, marlstone, sandstone, carbonate, granite and basalt. They are well rounded, angular or  
12 elongated and poorly sorted, they range from 2 cm to 90 cm in length. The matrix is poorly sorted it's composed  
13 of fine grained gravels, fine to very coarse grained sand, mud and carbonate cement. Subfacies F17b (Fig. 4K  
14 and Fig. 6) is a decimetric brownish yellow medium to fine -grained sandstone bed with erosional base and flat  
15 top, displaying planar cross stratification with some horizontal laminations and ripples. Subfacies F17c (Fig. 4L  
16 and Fig. 6), consists of a lenticular reddish brown, coarse-grained unit composed of two intervals. The lower  
17 interval (b) is a high erosively based clast-supported conglomerate bed ranging in thickness from 2 to 3 m. The  
18 clasts consist of pelite, marlstone, sandstone, carbonate, granite and basalt. They are well rounded to angular and  
19 poorly sorted, they range from 2 cm to 25 cm in length and they display ENE - WSW AB-plane type. The matrix  
20 is composed of fine to very coarse grained sand, fine grained gravels, bivalve shells debris, and occasionally  
21 carbonates cement. The upper interval is an erosively based decimetric allochemic sandstone unit which fines  
22 upward to very fine-grained sandstones and exhibits planar and through cross-stratified beds separated by  
23 erosional surfaces.

24 Facies F18 (Fig. 5A, 5B, and Fig. 6), is observed in the upper part of the upper Sandstone and pelitic  
25 Formation of Upper Oligocene to the Lower Miocene age (Fig. 3). It consists of alternating metric coarse-sandy  
26 micrite bed and decimetric to metric highly bioturbated muddy layer. The bed has an erosively undulating base  
27 with load cast, and an erosive top. It's composed of low-angle cross laminated sets separated by erosional  
28 surfaces and displays Ophiomorpha burrows, convolutes bedding, slumps and ball and pillow.

1 Facies F19 (Fig. 5C and Fig. 6), is identified in the upper part of the upper Sandstone and pelitic Formation  
2 of Upper Oligocene to the Lower Miocene age (Fig. 3). It consists of alternating metric coarse-sandy micrite bed  
3 and decimetric to metric highly bioturbated muddy layer. The bed has an erosively undulating base with load  
4 casts, and an erosive top and it's composed of stacked planar, quasi planar laminated tabular sets separated by  
5 reactivation surface or mud drap. The bedding may be disturbed by convolutes bedding and water escape  
6 structures.

7 Facies F20 (Fig. 5D and Fig. 6), occurs in the upper part of the upper Sandstone and pelitic Formation of  
8 Upper Oligocene to the Lower Miocene age (Fig. 3). It consists of alternating metric coarse-sandy micrite bed  
9 and decimetric to metric highly bioturbated muddy layer. The bed is erosively based with load casts and its upper  
10 surface is sharp and may display decimeter scale wavelength hummocks or ripples. Its internal structure shows  
11 sets of planar parallel lamina passing to micro-hummocky cross stratification expressed by successive lamina  
12 sets separated by low angle truncations surface and composed of parallel low-angle curved lamina which dome  
13 upward (hummocks) passing laterally into laminae that are concave upward (swaley).

14 Facies F21 (Fig. 5E and Fig. 6), is documented in the upper part of the upper Sandstone and pelitic  
15 Formation of Upper Oligocene to the Lower Miocene age (Fig. 3). It consists of alternating metric coarse-sandy  
16 micrite bed and decimetric to metric highly bioturbated muddy layer. The bed has an undulated erosive lower  
17 base with load casts, and generally contain 3 intervals (a, b and c from base to top). The lower interval (a) is  
18 limited to its top by an erosional surface and made up of successive couplets of thick (1-5cm) and thin (0,5-1cm)  
19 planar parallel micritic siltstone laminae limited each one to its upper surface by very thin mud layers (mm-  
20 scale) or mud drapes. The intermediate interval (b) is composed of symmetrical wave ripples passing to  
21 megaripple cross bedding. The upper interval (c) is characterized by micro-hummocky cross stratification  
22 expressed by successive lamina sets separated by low angle truncations surface and composed of parallel low-  
23 angle curved lamina which dome upward (hummocks) passing laterally into laminae that are concave upward  
24 (swaley).

25 Facies F22 (Fig. 5F and Fig. 6), is identified in the Si Moussa Formation of Middle Miocene age (Fig. 3). It  
26 consists of alternating metric sandy bar and decimetric to metric highly bioturbated muddy layer. The bar is  
27 composed of amalgamated lenticular metric cross stratified and cross laminated coarse-sandy micrite beds  
28 displaying sharp basal surfaces, low angle cross-stratified (less than 10°) laminations and sets of sigmoidal cross

1 laminations delimited by reactivation surfaces. The beds are disturbed by convolute bedding, slumps, and ball  
2 and pillow and may shows decimetric desiccation cracks at their top.

3

#### 4 Depositional environments reconstruction

5

#### 6 Sedimentary structure interpretation

7 The sedimentary structures which characterize the sedimentary facies identified in the Mrayt Group series  
8 revealed significant informations on the depositional and the post-depositional processes that control the  
9 sedimentation. The primary sedimentary structures observed indicate erosion and deposition under the interplay  
10 of waves, storms, tidal and fluvial currents.

11 The waves action is expressed by: symmetrical ripples (F1, F2, F10 and F21) and asymmetrical ripples (F1,  
12 F2, F3, F6, F10, F12, and F15 ) which present characteristics of wave-ripple bedding (De Raaf et al. 1977), such  
13 as: lateral variation in size and shape of the ripples in the same layer, offshooting and draping laminations  
14 expressed by foreset laminae which ascend and overlap the flank of the adjoining ripple, composite internal  
15 structure made up of an assemblage of differently structured, generally bidirectional lenses or multidirectional  
16 lenses, parallel undulated lamination, pinching and swelling laterally and passing to incipient lenses, small lenses  
17 of mud preserved in the trough of the ripple, swollen lens-like sets, undulating parallel laminations passing into  
18 cross laminations, ripple cross laminated layers which display unidirectional cross lamina concordant with the  
19 stoss side and irregular undulating lower bounding surface. Waves action is also expressed by low angle cross  
20 stratification (less than  $10^\circ$ ) in coarse sandy micrite (F18 and F22), which results from parallel seaward-dipping  
21 lamination in foreshore-backshore (Shahin et al. 2009).

22 Storm action is indicated by: hummocky cross stratification (F13), micro-hummocky cross stratification  
23 (F20, and F21) and quasi planar laminated tabular sets (F19). The Hummocky cross stratification (HCS) was  
24 introduced and described by Harms et al. (1975), it's produced, by unidirectional and oscillatory flow generated  
25 by storm events beneath the fair-weather wave base and above the storm weather wave base. It's widely  
26 recognized both in modern environments in the shoreface (Howard & Reineck 1981) and in the upper offshore  
27 (Swift et al. 1983). Micro-hummocky cross stratification occurs in open-coast intertidal flat, the HCS become  
28 smaller in a landward direction because of a decrease of wave size (Yang et al. 2006). Quasi planar laminated

1 tabular sets are considered as proximal tempestites deposited from storm wave-generated oscillatory flows or  
2 oscillatory-dominated combined flows (Jelby et al. 2019).  
3 Evidence of tidal current action is expressed by the existence of typical facies and structures as layers of  
4 sediments, periodically deposited in relation to daily and monthly tidal cycles and signature of reversing currents  
5 (Boersma 1969; Dalrymple et al. 1978; Visser 1980; Terwindt 1981; Allen and Homewood 1984; Mowbray and  
6 Visser 1984; Kreisa and Moiola 1986; Dalrymple and Makino 1989; De Boer et al. 1989; Tessier et al. 1989; Nio  
7 and Yang 1989; Dalrymple, 1992). Tidal bundle or mud couplet (F1, F11, F15, F16, and F21) indicates changes  
8 in current velocity and flow reversals related to daily tidal cycles. Sand lamina reflect alternating ebb and flood  
9 episodes known as diurnal inequality, coarser lamina are deposited by dominant tide current (thick lamination)  
10 and subordinated tide current (thin lamination) and mud drapes are formed during slackwater stages by  
11 deposition of suspended mud. Alternation of thick and thin tangential laminae (F4, F9, F16) or sigmoid laminae  
12 (F7, F11, F15, F16, F22) limited each one to its upper surface by very thin mud layer (F3, F8, F12, F20)  
13 corresponds to a tidal bundle related to daily tidal cycles. Sigmoid-shaped sets separated by reactivation surface  
14 or mud drapes and made up of successive mud couplets (F8) result of tidal lateral accretion of a large-scale  
15 bedform such as megaripples or sandwaves during a dominant tide. Stacked sets of thin laminae which thicken  
16 progressively from the bottom to the top and sets of thick laminae which thin progressively from the bottom to  
17 the top (F1, F6, F7, F10, F11, F12, F15, F16, F21) are considered as a tidal rhythmites. These microsequences,  
18 represent a vertical record of neap/spring tidal cycles fluctuations that occur during a lunar cycle. During spring  
19 tidal excursion is at maximum and during neap tide, tidal excursion is at minimum. Successive intervals  
20 exhibiting sigmoidal or tangential cross laminated cm-bundles, dipping in opposite directions (F11, F12) are  
21 generated by the reversing currents which can be developed in tidal environment. The cross laminated beds  
22 deposited during ebb tide dip in opposite direction of those formed during flood tide. Reactivation surface (F1,  
23 F7, F15, F19, and F22) is a minor erosion surface between cross-strata which results from partial erosion by  
24 reversing current during an asymmetrical tidal cycle. The lower bedform is eroded back by the reverse current  
25 and buried by a new advancing bedform.

26 Interbedded layers of fine sandstone and mudstone expressed by: 1) ripples with small lenses of mud  
27 preserved in the trough (F1, F2, F15), 2) Interbedded rippled sandy layers and continuous mud drapes  
28 overlapping the ripple troughs and crests (F1, F2) and 3) well preserved micritic siltstone or sandstones lenses,  
29 embedded within muddy layer (F2) are respectively flaser bedding, wavy bedding and lenticular bedding. These



1 sedimentary structures are characteristics of tidal deposits in intertidal zone and are related to tidal cycles, mud  
2 deposition is favored by the existence of slack tides (Reineck and Singh 1980; Dalrymple and Makino 1989). In  
3 the flaser bedding facies, ripple beds are deposited during periods of current activity and mud lenses result from  
4 mud in suspension when energy of currents decreases. Wavy beddings develop when preservation of mud is  
5 possible and lenticular bedding reflects more favorable conditions for deposition and preservation of mud than  
6 sand. Linguoid ripples (F5) and straight-crested ripples (F3 and F6) are generated in tidal flat by unidirectional  
7 current (Reineck and Singh 1980). Mud drapes (F1, F4, F6, F7, F10, F11, F12, F16, F19 and F21) may be found  
8 in various environments, their occurrence with typical tidal structures and facies is in favor of tidal origin. They  
9 result from deposition of concentrated suspended mud during the slack-water stage

10 Sedimentary structures related to fluvial currents are: asymmetric ripples characterized by a planar base and  
11 planar cross-lamination (F2, F5 and F8), flute casts (F10, F11, F12, F15, F16) and tool casts: groove casts (F9,  
12 F10, F11, F12), bounce cast (F9) and prod casts (F9, F10, F11). Flute casts is the molding of a flute mark, which  
13 is a tongue-shaped scour produced into mud by a turbulent flow of water. Tool casts are molding of tool marks  
14 which are produced by larger particles (e.g., pebbles and shell) on soft sediments under action of turbulent flow.  
15 Groove marks are caused when fragments are dragged along, prod casts and bounce casts are produced when  
16 fragments bounced along or hit the substrate. Flute casts and tool casts are commonly linked to turbidity currents  
17 in deep marine settings. However they can form also in the fluvial-to-marine transition zone under action of  
18 transitional flows whose turbulence results from the density differences between sediment-laden fresh and  
19 marine water. Fluvial current action is also demonstrated by the texture and the characteristics of the three  
20 conglomerate levels (Facies F17) such as the AB-plane type imbrications.

21 Post depositional and secondary sedimentary structures (Fig. 8) include desiccation cracks, water escape  
22 structures, load structures, soft sediment deformations and biogenic structures. Desiccation cracks (F1, F2, F3,  
23 F4, F5 F7, F9, F11, F13, and F22) are subaerial sedimentary structures which form when wet sediments dries up  
24 and contacts under evaporation processes. They occur in settings submitted to subaerial exposures: fluvial  
25 levees, shore of lakes, delta plain and tidal flat. Dish and pillar structures (F15 and F19) are water escape  
26 structures that form in unconsolidated sediments during stages of rapid deposition in deep sea fan and/or deltaic  
27 and fluvial systems (Lowe 1975).

28 Load casts (F18, F19, F20, F21) and flame structures (F10), form in response to deposition of layer of  
29 denser sediments (sand) over on a less-dense hydroplastic layer (mud), especially during high sedimentation rate.

1 The overloading lead to the sinking of the sand layer in the form of highly irregular protuberances and lobes  
2 (load casts) or projecting curved, pointed tongues of mud as wavy or “flame” shaped into the overlying sand  
3 (flame structures). Convolute beddings (F8 F10, F11, F12, F15, F16, F18, F19, and F22) are centimetric  
4 crumpling and folding of parallel laminae or foreset laminae of ripple bedding. They occur in fine grained soft-  
5 sediment in various settings from deep- marine to nearshore and fluvial environments, and they occur frequently  
6 are-in deltas and intertidal flats. They can be produced in more than one way (Reineck and Singh 1980 and  
7 reference therein): liquefaction, shearing action of currents, down-slope movement favored by the existence of a  
8 slope, high sedimentation rate, and seismic shaking.

9 Slump structures (Fig. 8) observed in Sandstone-pelitic Formation and Si Moussa Formation, consist of a  
10 metric size, complex fold patterns often overturned. They result from movement and displacement of  
11 unconsolidated sediments induced by high sedimentation rate, sliding down a slope, faulting and seismic  
12 shaking. Balls and pillows (F18, F22), may occur as rounded masses of coarse sediments (pseudonodules) in fine  
13 grained matrix or as isolated pillows with curved and deformed internal laminations in a sandstone layer. They  
14 result in unconsolidated sediment under a physical shock which causes instability and rupturing of the sediment  
15 layer, generally in relation with tectonics.

16 The trace fossils (Fig. 9) observed includes *Ophiomorpha* burrows (F10, F15, F16, and F18) Skolithos  
17 burrows (F15), Cruziana (F8 and F9), Ppsilonichus Y-shaped burrows (F3), Zoophycos (F16) and Paleodyction  
18 tunnels (F8 and F9). *Ophiomorpha* is considered as a part of the Skolithos ichnofacies (Seilacher 1967) and is  
19 produced by crustaceans such as shrimps (Frey et al. 1978) in nearshore and shallow marine depositional  
20 environments (Boggs 1995; Buatois and Mángano 2011), Skolithos belong to Skolithos ichnofacies (Seilacher  
21 1967) is produced by a variety of organisms and commonly associated with lower intertidal to shallow subtidal  
22 settings in moderate to high-energy conditions. Cruziana burrow belong to Cruziana ichnofacies is considered  
23 typical of subtidal above storm wave base, but was recognized in intertidal zone (Pandey et al 2014). Ppsilonichus  
24 may be produced by: decapod crustacean, shrimp or crab, it occurs in estuary to backshore sedimentary settings  
25 (Nesbitt and Campbell 2006). Zoophycos is considered as feeding or moving trace, it was associated for a long  
26 time with deep marine sediments, often turbidites. However it has been reported from shallow marine storm  
27 deposits (Zhang and Zhao 2016; Belghouthi et al. 2020) and nearshore settings (Knaust 2004). Paleodyction  
28 burrows consist of a regular hexagonal or polygonal network of tubular tunnels. They are commonly linked to  
29 deep -water Nereites ichnofacies (Seilacher 1967) and were identified in many flysch successions and at present

1 day abyssal environments. However they has been documented in prodelta environments, in relatively shallow  
2 epicontinental basin, and in mid -to -deep -shelf environments of Upper Triassic and Middle Jurassic in Iran  
3 (Fürsich et al. 2007), and in association of trace fossils belonging to Cruziana ichnofacies in the Devonian of  
4 Pennsylvania (Metz 2012). Y-Shaped burrows (Psilochinus) indicate a shallow marine coast (Frey et al. 1978).

5

## 6 Facies associations and facies sequences interpretation

7

8 The facies identified are grouped into three facies associations: Tide dominated estuary facies association, tide  
9 dominated delta facies association, and open-coast tidal flat facies association. (Fig.11). The estuary facies  
10 association is composed of a tidal flat sub-association (F1 F2, F3, F4,) and an estuary channel sub-association  
11 (F5, F6, F7). In the tidal flat sub-association, Facies F1 exhibits mud couplets, wavy bedding, flaser bedding,  
12 mud drapes and wave ripples. These sedimentary structures indicate deposition from tidal current and waves.  
13 Mud couplet reflects daily tidal cycles and mud drapes result from deposition of concentrated suspended mud  
14 during the slack-water stage. Occurrence of wavy bedding and flaser bedding is frequent in tidal setting where  
15 the slack tides favors mud deposition (Reineck and Singh 1980; Dalrymple and Makino 1989).

16 Facies F2 shows a vertical evolution from flaser bedding to lenticular bedding through wavy bedding which  
17 is considered as diagnostic of strongly tide influenced intertidal flats. Facies F3 comprises a slightly deformed  
18 interval and asymmetric ripples related to wave and tidal currents. Combined- flow and wave –induced structure  
19 and bedding characterize exposed tidal flat setting. The slight deformations of the lower interval may suggest a  
20 high sedimentation rate. Facies F4 represents deposition in a tidal creeck or gullie illustrated by erosively  
21 undulating base and tidal current induced structures such as: sets of parallel plane laminae, tangential cross  
22 laminated cm-bundles, reactivation surfaces and mud drapes. Successive tangential bundles and reactivation  
23 surfaces are related to diurnal inequality of tides.

24 In the estuary channel sub-association, Facies F5 consists of an erosionally based succession displaying a  
25 basal lag rich in mud pebbles, passing to silty micrite interval with unidirectional flow ripples which in turn is  
26 overlain by an interval with wave ripples. The top shows linguoid ripples and centimetric to decimetric  
27 desiccation cracks. This facies results from deposition within a distributary channel under the interplay of tide  
28 currents and waves. Mud pebbles form at least in two stages: 1) a breakage of muddy bed by desiccation during a  
29 dry periods, bioturbation or erosion by currents which results in the formation of muddy chunks and flakes, and

1 2) reworking of the intraformational clasts by storms or tidal currents and accumulation on the erosional surface  
2 as lag deposits. Linguoid ripples occur in tidal flat under unidirectional current (Reineck and Singh 1980).

3 Facies F6 comprises neap /spring tidal rhythmites mud drapes, wave ripples and desiccation cracks at its  
4 top. This facies is interpreted as a tidal point bar deposit under the interplay of tide currents and waves. Tidal  
5 point bar forms within active distributaries of the estuary and extends from shallow to supratidal settings, thus  
6 desiccation cracks occur during subaerial exposure stage.

7 Facies F7 displays neap spring tidal rhythmites, sigmoid-shaped sets made up of successive mud couplets,  
8 mud drapes, reactivation surface and desiccation cracks. It is interpreted as distributary channel fill, where tidal  
9 action is expressed by the most diagnostic structures of tidal origin: neap /spring tidal rhythmites, sigmoidal  
10 bundles, mud drapes and reactivation surface. The desiccation cracks result from subaerial exposure related to  
11 shallowing due to sedimentation and channel abandonment. Combined-flow and wave-induced structures and  
12 beddings suggests sedimentation in a tide dominated and wave influenced mixed tidal flat. The presence of  
13 desiccation cracks indicating repeated emergence. The existence of distributary and tidal channel fill is also  
14 supported by the existence of marine and littoral organisms such as benthic and planktonic foraminifera,  
15 *Calpionella* and bioclasts of: gastropods, bivalves, echinoderms, bryozoans and algae. Tide dominated estuary  
16 receive sediments both from the river at the head of the estuary and from adjacent shelf by tidal currents.

17 The delta facies association includes a lower delta plain sub-association (F3, F4) a tide dominated delta  
18 front platform sub-association (F9, F10, F11 F12, F13 F14, F15, F16, and F17), and a prodelta (F8). In the delta  
19 plain sub-association, facies F3 suggests deposition in tidal flat under combined- flow and wave action and  
20 facies F4 represents tidal creek fill. In the front delta platform sub-association, Facies F9 display an erosional  
21 base with tool casts (grooves casts, prod casts and bounce casts), Paleoduction tunnels, tangential cross  
22 laminations and desiccation cracks at its upper bounding surface. This facies result from transitional flows in the  
23 front delta slope. Tangential cross laminations are induced by unidirectional flow. Tool casts can form in such  
24 fluvial-to-marine transition zone where the interaction of sediment-laden freshwater river flux and tidal currents  
25 generates turbulent eddies and strong shears Paleoduction has been documented in deltaic environments, in  
26 relatively shallow epicontinental basin. The desiccation cracks at the top of the bed are related to subaerial  
27 exposure episode due to swallowing of the setting.

28 Facies F10 and F11 has an erosive base exhibiting prod casts (F10) and flute casts (F10, F11) induced by  
29 transitional flows whose turbulence results from the interaction of fluvial and marine process. Gravity-driven

1 transport may occurs when river are discharging peak sediment loads onto an energetic marine environment.  
2 This mode of sediment transport has been highlighted in several deltas studies. (e.g. Wright and Friedrichs  
3 2006). Their internal structure which can be affected by flame (F10 ) and convolute beddings ( F10, F11) is  
4 made up of alternating wave ripples and tidal sedimentary structures such as: neap spring tidal rhythmites, wavy  
5 bedding, sigmoidal cross laminations, opposite directions of fore set laminations in adjacent layers, reactivation  
6 surfaces. The upper surface of these facies may shows mud pebbles (F10, F11) and decimetric-scale desiccation  
7 cracks (F11) and the base of F10 base exhibits Ophiomorpha burrows (F10). The presence of mud pebbles  
8 indicates an accumulation at the top of beds during episodic storm events. F12 displays alternating wave ripples  
9 which may be disturbed by convolutes bedding and tidal structures: neap spring tidal rhythmites, tangential cross  
10 laminated cm-bundles dipping in opposite directions in adjacent layers and mud drapes. This facies result from  
11 the interplay between tidal currents and waves.

12 Facies F10, F11 and F12 are interpreted as tidal sand ridges deposits which developed in the delta front  
13 platform. This part of the deltaic system is controlled by the interplay between river discharges and fluvial  
14 sediment load and marine processes: tides, waves, and episodic storms. The vertical succession of sedimentary  
15 structures indicate rapid transition from subtidal to intertidal setting, desiccation cracks are related to subaerial  
16 exposure period due to swallowing of the setting. The presence of Ophiomorpha burrows is also indicative of a  
17 high energy sublittoral or shoreface environments. This trace fossil occurs from littoral to shallow-marine  
18 paleoenvironments (Buatois and Mangano 2011).

19 Facies F13 corresponds to a storm event deposit as indicated by its geometric characteristics: erosional  
20 undulating base and erosive top exhibiting metric scale wavelength hummocks, and its internal structures  
21 expressed by metric scale hummocky cross stratification. Decimetric desiccation cracks and soft pebbles at the  
22 top indicate period of subaerial emergence.

23 Facies F14, F15, F16 and F17 represents channel fill deposits at the mouth area of front delta. Facies F14,  
24 F15, F16 have in common a highly erosive base with flute casts and an interval corresponding to a lenticular  
25 fining upward microconglomerate which may comprise tangential cross-stratification. In Facies F15 and F6, this  
26 interval is surmounted by a finning upward sequence showing grading from allochemic sandstones which may  
27 be affected by dish and pillar structures and convolutes bedding (F15) into micritic siltstone or silty micrite. The  
28 sequence in F15 exhibits waves rippled and tidal structures: mud couplets tidal rhythmites reactivation surfaces,  
29 sigmoidal tidal bundle and flaser bedding as well as mud pebbles, and Ophiomorpha and Skolithos burrows at its

1 top. The sequence in F16 displays only tidal structures: neap spring tidal rhythmites, sigmoidal bundle, mud  
2 drapes and reactivation surface and Zoophycos, Ophiomorpha and Skolithos burrows traces at its top.

3 Facies F14 is interpreted as being a channel fill deposit from unidirectional turbulent flow. Facies F15 and  
4 F16 record different stages of channel initiation and fill, scouring, flute cast and normal grading of the lower  
5 interval are related to unidirectional turbulent flow. The filling of the F15 channel was made first under action  
6 tidal current and with shallowing upward due to sedimentation, the filling continued with waves. In the case of  
7 F16 filling was made only by tidal currents. The existence of nearshore to marine organisms and shell fragments  
8 in facies F14, F15, and F16 confirms the intrusion of marine and coastal currents in the channels. Ophiomorpha  
9 and Skolithos burrows belong to skolithos ichnofacies (Seilacher 1967) which is diagnostic of nearshore and  
10 shallow marine depositional environments. Zoophycos has been reported from shallow –marine storm deposits  
11 (Zhang and Zhao 2016; Belghouthi et al. 2020) and nearshore settings (Knaust 2004). Dish and pillar structures  
12 consist of fluid escape structures which results of quick packing due to high sedimentation rate. Convolute  
13 bedding are common in front delta and prodelta settings, they may form during gravity-driven flows or tectonic  
14 events.

15 Facies F17 is interpreted as fluvial deposits based on the dimension, the lithology, the composition, the  
16 texture and the sedimentary structures that characterize fluvial facies (Miall 1992). The shape of the clasts  
17 underlines a short transport distance. The absence of sedimentary structure and fabric as well as the poor sorting  
18 of the massive polymictic, texturally immature matrix supported conglomerate (Subfacies F17a), suggest  
19 deposition by gravity flow. Fine -grained sandstone bed (Subfacies F17b) might have resulted from deposition  
20 by vertical accretion on the top of channels sand bars during low flow régime. Clasts-supported conglomerate  
21 unit (Subfacies 17c) is interpreted as channel lag deposits, based on its highly erosive base, lenticular shape, and  
22 texture especially the AB-plane type imbrications of the clasts. The coarse sandstones exhibiting planar and  
23 cross-stratified beds separated by erosional surfaces may be attributed to vertical accretion during lower flow  
24 regime, or to the migration of sand dunes and transvers bars in shallow water stream channel. These subfacies  
25 result from fluvial discharges in response to flooding stages and reactivation of detrital inputs due to tectonic  
26 events and uplift of the source area. Marine to nearshore bioclasts such as bivalve shells of the matrix of the clast  
27 supported conglomerate and the coarse sandstone, confirm deposition at the mouth of delta submitted to flood  
28 tides.

1 Facies F8 consist of predominant muddy deposit with centimetric alternation of silty micrite displaying  
2 planar parallel laminations or tabular cross-laminations that may be disturbed by convolutes bedding, and intense  
3 bioturbation. This facies can be formed in an offshore or in a prodelta this last hypothesis is the most probable  
4 because of its association with deltaic facies at the base of upward coarsening sequence. Convolutes bedding are  
5 frequent in such setting and may be induced by gravity driven transport in the delta slope or under high rate of  
6 sedimentation. Intense bioturbation indicates a low-energy setting with normal oxygenated conditions. The  
7 presence of Paleoduction tunnels has been documented in prodelta environments (Fürsich et al. 2007).

8 In the open-coast tidal flat facies association, Facies F18 is interpreted as nearshore sand bar based on low-  
9 angle cross laminated sets separated by erosional surfaces. Low-angle cross laminated result from mega ripples  
10 migration and may be generated by waves processes during fair weather periods (Wright and Short 1984).  
11 Occurrence of Ophiomorpha trace fossil is consistent with nearshore environments. Load casts may results from  
12 high sedimentation rate. Convolutes bedding, ball and pillow and slumps may be induced by tectonics.

13 Facies F19 is interpreted as proximal tempestite deposited from storm wave-generated oscillatory-dominant  
14 combined flows (Jelby et al. 2019) and tidal currents, based on the existence of erosional limits, quasi planar  
15 laminated tabular sets, reactivation surfaces and mud draps. Association of proximal tempestites and tidal  
16 structures are in favor of a cyclic deposition by storm and tide currents in an open coast tidal flat. Water escape  
17 structures and convolutes bedding which may affect this facies, might have been induced by a high  
18 sedimentation rate or storm waves. Soft -sediment deformation structures are well documented in tempestites  
19 and interpreted as the result of liquefaction triggered by the stress induced by storm waves (Jelby et al., 2019 and  
20 references therein).

21 Facies F20 is considered as storm deposit in intertidal flat based on the existence of erosional bounding  
22 surfaces, planar parallel lamina and micro-hummocky cross stratification. Micro-hummocky cross stratification  
23 occurs in open-coast intertidal flat, the HCS become smaller in a landward direction because of a decrease of  
24 wave size (Yang et al. 2006). Load casts express a high sedimentation rate.

25 Facies F21 consist of coarse-sandy micrite bed displaying mud couplet, wave ripples passing to megaripple  
26 cross bedding and micro-hummocky cross stratification. This facies is generated in the intertidal zone under the  
27 tide, waves and storm action.

28 Facies F 22 corresponds to a nearshore sand bar generated by fair weather wave and ebb or flood delta  
29 which developed in tidal inlet by tidal current. Waves signature is expressed by the existence of low angle cross-

1 stratified (less than 10°) laminations. Influence of tidal currents is recorded by the sets of sigmoidal cross  
2 laminations delimited by reactivation surfaces. Occurrence of decimetric desiccation cracks at the top of beds  
3 suggests sedimentation in nearshore setting submitted to subaerial exposure. Convolute bedding, ball and pillow  
4 and slumps are probably induced by tectonics.

5 Open-coast tidal flat recorded by Facies association (F18 F19, F20, F21, and F22) developed under action of  
6 tides, fair weather waves and storm action. It corresponds to a sandy open coast tidal flat in the classification of  
7 Daidu (2012) which is characterized by: 1) abundance of storm-generated structures, 2) scarcity of tidal-channel  
8 deposits and 3) abundance of structures created by combined flows or the interactions of waves and tides.  
9 According to this author, such depositional environment is common in the open-mouth estuaries of small river  
10 and the adjacent strand plain.

11

## 12 Discussion

13

14 The Mrayt Group deposits have been previously described as siliciclastic sediments: quartzarenite and  
15 sublitharenites (Tejera de Leon 1993) the petrographic analysis of thin sections performed in this study, has  
16 shown that the sediments are not siliciclastic deposits but rather mixed siliciclastic/carbonate components. The  
17 petrofacies recognized according to Mount classification (1985) are: silty micrite, micritic siltstones, micritic  
18 sandstones, sandy micrite, and allochemic sandstones. They are very similar to those observed within the Eocene  
19 to Miocene sedimentary series outcropping in the North Western Rif (Hamoumi 1995b; Hamoumi et al. 1995;  
20 Ouldchalha et al. 1995; Salhi et al. 1995). These new findings are even more important than mixed siliciclastic /  
21 carbonate rocks in the Rif belt are not well encoded. The tendency has been to ignore the mixed composition and  
22 to consider them as pure siliciclastic or pure carbonate rocks and to use carbonate or siliciclastic classifications  
23 which results in wrong nomenclatures. Precise petrographic analysis and classification are necessary for accurate  
24 naming and classifying sedimentary rock which is in turn essential to reconstitute provenance, tectonic setting,  
25 climate, transport and sedimentation processes, depositional environments and diagenetic history. They are also  
26 fundamental tools in hydrocarbon exploration and engineering.

27 The compositional mixing indicates contemporaneous accumulation and sediment supply from both intra-basinal  
28 and extra-basinal sources. The intra-basinal components: shell fragments, algae glauconitic peloids  
29 rhombohedral crystals of dolomite and mud clasts, suggest nearshore to shallow marine depositional setting



1 submitted to flood tides. The extra-basinal source that provides the siliciclastic components and detrital  
2 carbonates, may corresponds to the geological sections outcropping along the African margin which consists of  
3 Paleozoic basement of detrital dominance, folded, metamorphosed and granitized during Hercynian orogeny and  
4 its cover, the Meso-Cenozoic terranes, which are essentially carbonates. The presence of Cretaceous benthic  
5 foraminifera of the genus *Orbitolina* and other micritized foraminiferal test argues their provenance from the  
6 Meso-Cenozoic sediments. This hypothesis is supported by the results of palaeocurrents analysis carried out in  
7 this work that indicate a transport path from SSE to NNW, and those of previous works (Cazzola and Critellis  
8 [1987](#); Morley [1992](#); Tejera de Leon [1993](#)).

9 Previous works have proposed deposition of the Mrayt Group successions in marine (distal shelf and  
10 continental slope) of foredeep basin. They interpreted as a sedimentary prism adjacent to the outer edge of a  
11 storm dominated platform, which passes to deep sea fan system (Raissouni et al. [2008](#)), or as synorogenic  
12 turbidites referred to deep sea fan and reworked and redeposited slope flows in an abyssal plain (Morley [1992](#);  
13 Tejera de Leon [1993](#)). Sedimentary facies reconstruction and interpretation performed in this work indicates that  
14 deposition of Mrayt Group sediments was realized in littoral and shallow marine environments: tide dominated  
15 estuary, tide dominated delta and open-coast tidal flat.

16 In these depositional environments, sedimentation took place under complex hydrodynamics strongly  
17 influenced by river discharge, tidal currents, waves and storms action. Evidence of tidal current is expressed by  
18 unique sedimentary structures and facies that can only be produced by tides such as: layers of sediments,  
19 periodically deposited in relation to daily and monthly tidal cycles and signature of reversing currents (Boersma  
20 [1969](#); Dalrymple et al. [1978](#); Visser [1980](#); Terwindt [1981](#); Allen and Homewood [1984](#); Mowbray and Visser  
21 [1984](#); Kreisa and Moiola [1986](#); Dalrymple and Makino [1989](#); De Boer et al. [1989](#); Tessier et al. [1989](#); Nio and  
22 Yang [1989](#); Dalrymple [1992](#)). The waves action is indicated by typical wave-generated symmetric and  
23 asymmetrical ripples (De raaf et al. [1977](#)) and low angle cross stratification (Shahin et al. [2009](#)). The storm  
24 signature is expressed by hummocky cross stratification (Harms et al. [1975](#)), micro-hummocky cross  
25 stratification, (Yang et al. [2006](#)) and quasi planar laminated tabular sets (Jelby et al. [2019](#)). The fluvial action is  
26 recorded by current asymmetric ripples, flute casts and tool casts (groove casts, bounce casts and prod casts) and  
27 the the AB-plane type imbrications of the pebbles of the conglomerates. Nearshore environments are also  
28 suggested by: i) the presence of Skolithos and Ophiomorpha burrows considered part of the Skolithos  
29 ichnofacies (Seilacher [1967](#)), ii) Psilochinus Y-shaped burrows which indicate a shallow marine coast (Frey and

1 Pemberton 1978), iii) desiccation cracks indicating repeated emergence and iv) the presence of shell debris and  
2 abundant mud clasts in the floor the channels.

3 Sedimentation occurred in “the Maghrebian basin” defined by Bouillin (1986), extending between the  
4 North African margin and the Internal zones domain during the Mesozoic-Paleogene interval (Wildy 1983),  
5 under the interplay of tectonics and subsidence, eustacy, climate and sediment supplies. Evolution of the tectonic  
6 regime was guided by the complex subduction events and associated collisions between the African and Eurasian  
7 continental plates during the late Mesozoic and Cenozoic (Dewey et al. 1989; Srivastava et al. 1990; Leprêtre et  
8 al. 2018 and references therein). After the Early Eocene Climatic Optimum (EECO), the evolution of the  
9 Cenozoic climate recorded gradual trends of warming and cooling (Zachos et al. 2001). Following the Ypresian  
10 high sea level, Cenozoic period was marked by short-term sea level fluctuations due to the increasing influence  
11 of glaciation. (Haq et al. 1987).

12 Three depositional system intervals are recognized in the Mrayt Group successions from Early Eocene to Mid  
13 Miocene: tide dominated estuary, tide dominated delta and open-coast tidal flat. The first interval extended from  
14 Early to Middle Eocene, it records a tide dominated estuary system composed of a tidal flat and estuary  
15 channels. The tidal flat is characterized by tidal rhythmites and fining upward heterolithic successions showing  
16 regular changes vertically from flaser bedding through wavy bedding and lenticular bedding, (F1 and F2),  
17 surmounted by tidal creek or gully ( F3 and F4). The estuary channel sub-association comprises, distributary  
18 channel fill (F5 and F7), tidal point bar (F6).

19  
20 The Mrayt Group Eocene estuary system is a coastal plain estuary type where tidal action is expressed by  
21 the most diagnostic structures of tidal origin. Tide dominated estuaries are those in which tidal currents play  
22 dominant role at the mouth (Dalrymple et al. 2012). They form generally in shelves that are large enough to  
23 amplify the oceanic tidal wave. Initiation and development of estuarine system depends on three principal  
24 factors: rise in sea level, climate and subsidence. According to Dalrymple et al. (1992) an estuary is a  
25 transgressive coastal environment at the mouth of a river, that receives sediment from both fluvial and marine  
26 sources and that contains facies influenced by tide, wave and fluvial processes. The climate controls the amount  
27 of precipitation and therefore the fluvial flow regime as well as the nature and quantity of the sediment supplies.  
28 Recent estuaries occur in temperate and tropical regions which are characterized by frequent and abundant rains

1 and the existence of large rivers. Subsidence is necessary for the preservation of tidal deposit in as much as a part  
2 of the sediments deposited by a tidal current if not all may be eroded by the opposite tidal current.

3 The Mrayt Group estuary system was initiated by the drowning of an existing river valley during the Early  
4 Eocene (Ypresian) sea level raise (Haq et al. 1987). Development of this estuarine system was favored by the  
5 subsidence and a warm and humid climate. After the end of the Paleocen-Eocene Thermal Maximum (PETM) at  
6 56 million years ago, the Eocene climate began with a warming (Zachos et al. 2001). According to Brinkhuis et  
7 al. (2006) the warm greenhouse conditions of the Early Paleogene period (55-45 Myr ago) probably increased  
8 precipitation. Moreover, the climate in the Sahara during the Eocene would have been humid and warm (Swezey  
9 2009).

10 The Mid-Upper Eocene gap in the Mrayt Group succession could be explained by erosion or by an  
11 interruption in deposition. This last hypothesis seems the most plausible. Non deposition may be attributed to the  
12 combination of the effects of lowering in eustatic sea level and tectonic uplift. Major sea level falls occurred at  
13 the latest Ypresian and the latest Bartonian (Haq et al. 1987). Moreover, the Middle Late Eocene kinematic  
14 reorganization related to the strong coupling between the Eurasian, Iberian and African plates resulted in the  
15 development of intracontinental belts and compressive deformation at the scale of the west Mediterranean region  
16 (Leprêtre et al. 2018 and reference therein ).

17 The second interval records the development of a tide dominated deltas during Early Oligocene to Early  
18 Miocene period. Recognition of these depositional systems is based on the existence of three genetically linked  
19 facies and facies association in the same succession: lower delta plain facies association, delta front platform  
20 facies association and prodelta facies. The lower delta plain sub-association includes tidal flat (F3) and (tidal  
21 creek or gully (F4). The tide dominated delta front platform sub-association includes: deposit of transitional  
22 flows in the front delta slope (Facies F9), tidal sand ridges (Facies F10, F11 and F12), channel fill deposits at the  
23 mouth area of front delta (Facies F14, F15, F16 and F17) and a prodelta facies (F8).

24 Recognition of tide dominated delta is also based on the typical criteria commonly admitted for delta  
25 identification and the type of delta discrimination. 1) Coexistence of sedimentary structures and facies indicating  
26 a combination of the effects of river discharge, wave, storm and tidal processes 2) Thick predominately clastic  
27 successions which pass from subaqueous (offshore and shoreface) facies upwards into subaerial (intertidal flat  
28 and fluvial channel). 3) Typical coarsening upwards sequence from prodelta to distributary channel and sand  
29 bars interfingered with interdistributary muds. 4) Repeated progradation within a depocenter. 5) Occurrence of

1 the coarsest sediments in the boundary zone between the delta -front platform and slope and in the prograding,  
2 distributary -mouth channel bars.

3 Tide dominated delta are those where tide currents are the dominant process controlling sediment dispersal  
4 (Galloway 1975). The criteria which serve to distinguish tide dominated delta from the other deltaic systems are:  
5 the existence of typical tidal sedimentary structures, sedimentary facies and sequences in the mid to upper part of  
6 the delta front, the distributary tidal mouth bar and the lower delta plain successions. These tidal indicators are:  
7 mud couplets, neap spring cycle, tidal rhythmites, bidirectional structures, reactivation surfaces, upward fining  
8 succession, regular changes vertically from flaser bedding through wavy bedding and lenticular bedding, tidal  
9 creek fill, distributary channel fills, tidal sand ridges, The criterion which serves to distinguishes tide dominated  
10 delta from other tidally influenced settings is the “S” shaped sedimentary succession that tends to be heterolytic  
11 and both coarsening and fining upward (Goodbread and Saito, 2012). Additional criteria in favor of deltaic  
12 interpretation are: 1) decimetric desiccation cracks and soft pebbles which indicate period of subaerial  
13 emergence, 2) convolutes bedding which may be induced by gravity driven transport in the delta slope or under  
14 high rate of sedimentation. 3) Intense bioturbation which indicates a low-energy setting with normal oxygenated  
15 conditions, 4) mixing of marine to brackish fauna with detrital sediments from hinterland due to saltwater  
16 transport by flood tides.

17 The direction of flow in this delta has been reconstructed based on by the paleocurrent measurements of 48  
18 flute casts identified in all the studied outcrops. The paleocurrent flow as revealed by the rose diagram indicates  
19 a transport path from SSE to NNW (Fig. 10) and is consistent with that proposed by the previous works (Cazzola  
20 and Critelli 1987; Morley 1992; Tejera de Leon 1993). Other deltaic systems have been recognized in sections of  
21 the same age in the North Western Rif (Hamoumi et al. 1995; Oueldchelha et al. 1995), which was considered by  
22 previous work as deep sea fan deposits.

23 The initiation and the development of the Mrayt Group deltas were favored by the combination of major  
24 factors: tectonics and subsidence, sea level fluctuations, climate and sediments supplies. Delta construction was  
25 favored by the creation of depocenters induced by tectonics and subsidence. An Oligocene to Early Miocene  
26 extensional phase representing one of the two periods of strong mechanical coupling between Africa and  
27 Europe/Iberia plates, is recorded (Leprêtre et al. 2018 and references therein). Evidence for the tectonic control  
28 during sedimentation is revealed by: syndimentary faults and soft sediment deformations (slumps, ball and  
29 pillow). Tectonic activity and uplift in the drainage basin is attested by large amount of detrital sediment supplies

1 induced by rejuvenation of the source areas following the end Eocene tectonic uplift in relation to the major pre-  
2 oligocene compressional event (Leprêtre et al. 2018 et references therein). It's also confirmed by the presence of  
3 sedimentary structures induced by rapid deposition and increase in sedimentation rates (water escape structures,  
4 load structures). Most present day tide dominated delta is situated in tectonically active regions (Goodbread and  
5 Saito 2012).

6 Delta formation was also favored by the relatively higher sea level recorded at the Early Rupelian (Haq et al.  
7 1987). Delta confined to the shelf in shallow water is deposited during times of relatively high sea level. In  
8 addition, tide dominated delta are more generally highstand features as adequate tidal energy is less well  
9 developed during lowstand (Goodbread and Saito 2012). The climate plays a major role in both the catchment-  
10 based forcing of sediment production and fluvial transport. Tropical climatic conditions in the Eocene has  
11 changed warm subtropical in the Oligocene. The gradual cooling which occurred during the Eocene - Oligocene  
12 transition at 34 million years ago (Zachos et al. 2001), should be associated with humidity and precipitation as  
13 indicated by: i) the importance and quantity of detrital supplies and ii) alteration affecting feldspar and micas as  
14 well as small size and lower frequency of feldspar. Moreover, it appears that during Oligocene, north-flowing  
15 fluvial systems became a predominant feature across some parts of northern Africa during this time. (Swezey  
16 2009) and North Africa was closer to the equator (Guiraud et al. 2005).

17

18 Described facies and facies association occur in three progradational vertically stacked stratigraphic units.  
19 Each unit shows an upwards coarsening succession from the prodelta mudstones, gradationnaly overlain by delta  
20 front tidal bars, followed by erosively based distributary channels. The uppermost unit is overlain by lower delta  
21 plain deposits. Development and evolution of these stratigraphic units were realized by repeated progradation  
22 and abandonment within a depocenter dictated by fluctuations in sediment supply, subsidence and sea-level. In  
23 the first two units, deltaic deposition occurs during the Rupelian relatively high sea-level (Haq et al. 1987). The  
24 higher stratigraphic unit is composed of three sub units, the lowers one is an upwards coarsening succession  
25 similar to the first units with prodelta deposits gradationnaly overlain by delta front channel fill and tidal bars.  
26 The second subunits is composed of stacked metric erosively based distributary channels and the third subunit is  
27 a lower delta plain succession.

28 Progradation of the first subunit was favored by tectonic and climate, the major sea level fall which  
29 occurred near the Rupelian-Chatian boundary ( Haq et al 1987), was compensated by compressive tectonics. A

1 significant compressional event was recorded in the tell Rif system during pre -Late Oligocene (Leprêtre et al.,  
2 2018 and references therein). In addition, the tectonics allowed the source reactivation. Deposition of the second  
3 subunit of the mouth areas is related to the development of an extensive fluvial systems which was favored by: i)  
4 the persistence of decline in sea level, forced regression of the shoreline drives delta progradation and potentially  
5 downward incision, ii) continued tectonic uplift of the hinterland and iii) enough rainfall, north-flowing fluvial  
6 systems was a predominant feature northern Africa in during the Oligocene (Swezey 2009). The third subunit  
7 correspond to the lower delta plain reflect deposition during rising relative sea level and creation of  
8 accommodation space behind the delta front. This transgression would have been coincident with the higher  
9 eustatic sea level (Haq et al. 1987) and generally warm climate that characterized the late Middle Miocene  
10 (Zachos et al. 2001).

11 The third interval is a sandy open-coast tidal flat during Early Mid Miocene. Recognition of this  
12 depositional system is based on the existence of rhythmic alternation of nearshore sand bars generated by fair  
13 weather waves (facies F18 and F22), storms (facies F20) storms and tidal currents (facies F19) and wave and  
14 tidal current (facies F21). Nearshore environment is also indicated by centimetric to decimetric desiccation  
15 cracks and Ophiomorpha burrows. Sandy open-coast tidal flats are common in the open-mouth estuaries of small  
16 river and the adjacent strand plain (Daidu 2012). This stratigraphic unit expresses the abandonment of the  
17 deltaic sedimentation and the installation of a wave storms and tide dominated open tidal flat. It coincides with  
18 relatively high sea levels recorded during Aquitanian, Burdigalian, Langhian and Lower Serravallian (Haq et al.  
19 1987).

20 Sedimentation was favored by enough rainfall to support the development of extensive fluvial systems in  
21 the hinterland. The global cooling induced by the establishment of the major ice-sheet on Antarctica (Frakes et  
22 al. 1992) was interrupted by warm intervals. A warming trend was recorded from the Lower Miocene to the Mid  
23 Miocene where the warm phase peaked in the climatic optimum (Zachos et al. 2001). Sediment supplies have  
24 been ensured by continued tectonic uplift along the northern Africa margin, related to the change in motion of  
25 the African plate during Early Miocene (Leprêtre et al. 2018 and references therein). The rate of sedimentation  
26 was probably important as demonstrated by the existence of water escape and load casts structures.  
27 Sedimentation was favored also by the fact that accommodation outpaces the sedimentation rates at the coastline.  
28 Tectonic was active during sedimentation as indicated by soft sediment deformations as slumps, ball and pillow  
29 and convolutes bedding.

1  
2  
3  
4  
5  
6  
7  
8  
9  
10  
11  
12  
13  
14  
15  
16  
17  
18  
19  
20  
21  
22  
23  
24  
25  
26  
27  
28  
29

## Conclusion

This work presents new insight concerning the nature and composition of the sediments, the depositional environments and the factors that have controlled sedimentation for the Eocene-Miocene Mrayt Group in North-Western Rif (Morocco). The petrographic study reveals, for the first time, the mixed siliciclastic/carbonate composition of the deposits and their nomenclature: silty micrites, micritic siltstones, micritic sandstones, sandy micrite, and allochemic sandstones. They reflect sediment supply from an intra-basinal source that provides exoskeletons, glauconitic peloids, algae and rhombohedral crystals of dolomite and mud pebbles and extrabasinal sources, which correspond to the metamorphosed and granitized Paleozoic basement, and its Mesozoic cover outcropping in the northern African margin. Detrital fraction characteristics indicate also rapid erosion from a young and high relief continental source and a short transport and rapid deposition.

Twenty two sedimentary facies that have never been described before are identified, and based on their succession and association a new interpretation of depositional processes and depositional systems are proposed. The paleoenvironments of the Mrayt Group are interpreted as littoral and shallow marine settings: tides-dominated estuary, tides-dominated delta systems and open coast tidal flat, under complex hydrodynamics strongly influenced by river discharge, tidal currents, waves and storms action. Sedimentation occurred in “the Maghrebian basin” under the interplay of: i) tectonics related to the Cenozoic collision of the African and Eurasian continental plates, ii) Cenozoic alternation of warm climate and cooling due to the increasing influence of Antarctica glaciation, iii) sediments supplies induced by rejuvenation of sedimentary sources and iiiii) sea level fluctuation related to the advance and retreat of ice-sheet on Antarctica.

This work brings also additional insights such as the occurrence of Paleodictyon trace fossils in prodelta environment, Zoophycos trace fossils in nearshore settings and Cruziana burrow in the intertidal zone. The first two trace fossils are normally associated with deep-sea flysch settings and Cruziana is considered typical of subtidal above storm wave base. In addition to these new findings, this work is important for increasing our knowledge about ancient tides dominated deltas that is less investigated in comparison to the other deltaic systems (waves or river dominated) and its responses to sea level changes and tectonics. Last but not least, it consists an essential contribution for a better knowledge of North Western Rif belt and the the peri-Mediterranean alpine chain.

1   **References**

2

3           Abdelkhaliki L (1997) Evolution tectono-sédimentaire des dépôts gravitaires dans le Prérif interne et l'unité  
4 du Habt (Rif externe occidental, Maroc) : mise en place dans les bassins néogènes d'avant-fosse. Thèse 3ème  
5 cycle, Univ. Md V, Rabat, 176 p

6           Allen P, Homewood P (1984) Evolution and mechanics of a Miocene tidal sandwave: *Sedimentology*, v.  
7 31: 63- 81

8           Andrieux J (1971) La structure du Rif central. Etude des relations entre la tectonique de compression et les  
9 nappes de glissement dans un tronçon de la chaîne alpine. *Notes et Mém. Serv. Géol.,Maroc*, 235

10          Belghouthi F, Wetzel A, Zouari E, Jeddi RS (2020) Zoophycos in storm affected Maastrichtian deposits ( N  
11 Tunisia) *Ichnos* 27

12          Boersma J R (1969) Internal structure of some tidal mega-ripples on a shoal in the Westerschelde estuary,  
13 the Netherlands: report of a preliminary investigation. *Geol. Minjnb, Amsterdam*, 48: 409-414

14          Boggs S (1995) *Principles of Sedimentology and Stratigraphy*, 2nd Edition. Prentice Hall Inc.

15          Bouillin J (1986) Le "bassin maghrebin"; une ancienne limite entre l'Europe et l'Afrique a l'ouest des  
16 Alpes. *Bulletin de la SocieteGeologique de France*, vol.II, issue.4, 547-558

17          Brinkhuis H, Schouten S, Collinson ME, Sluijs A, Damsté JSS, Dickens GR, Huber M, Cronin TM,  
18 Onodera J, Takahashi K, Bujak JP, Stein R, Van der Burgh J, Eldrett JS, and the Expedition 302 Scientists (   
19 2006) Episodic fresh surface waters in the Eocene Arctic Ocean: *Nature*, v. 441, no. 7093, p. 606-609.

20          Buatois L, Mangano M G (2011) *Ichnology: Organism-Substrate Interactions in Space and Time*.  
21 *Geological Magazine* , 149 : Issue 4 , pp. 750.

22          Cazzola C, Critellis S (1987) Litostratigraphia e petrologia delle quarzoareniti torbidiche oligomiocenic  
23 di Asilah (Catenadel Rif, Marocco nord-occidentale). *Miner.Petrogr.Acta XXX*: 203-226

24          Collinson (1969) The sedimentology of the Grindslow shales and the Kinderscout grit; a deltaic complex in  
25 the Namurian of northern England , *Journal of Sedimentary Research* 39 (1): 194–221

26          Daidu F (2012) *Principles of Tidal Sedimentology*, Ed. Springer, 187-222

27          Dalrymple RW (1992) Tidal depositional systems. In: Walker, R.G., James, N. P., (eds). *Facies Models:*  
28 *Response to Sea Level Change*. Geological Association of Canada, St. John's, 195-218.



- 1 Dalrymple RW, Knight RJ, Lambiase JJ (1978) Bedforms and their hydraulic stability relationships in a  
2 tidal environment, Bay of Fundy, Canada. *Nature*, 275: 100-104
- 3 Dalrymple RW, Makino Y (1989) Description and genesis of tidal bedding in the Cobequid Bay–Salmon  
4 river estuary, Bay of Fundy, Canada. In: Taira, A., Masuda, F. (Eds.), *Sedimentary Facies of the active Plate*  
5 *Margin*. Terra Publishing, Tokyo: 151 – 177
- 6 Dalrymple RW, Zaitlin BA, Boyd RA (1992) A conceptual model of estuarine sedimentation. *J Sediment*  
7 *Petrol* 62:1130–1146.
- 8 Dalrymple RW, Mackay D A, Ichaso A A, Choi K S (2012 ) Processes, Morphodynamics, and Facies of  
9 Tide-Dominated Estuaries. In R.A. Davis, Jr. and R.W. Dalrymple (eds.), *Principles of Tidal Sedimentology*, 79.  
10 Springer Science and Business Media B.V. 2012
- 11 De Boer P, Oost A, Visser MJ (1989) The Diurnal Inequality of the Tide as a Parameter for Recognizing  
12 tidal Influences. *Journal of Sedimentary Petrology* 59: 912-921
- 13 De Raaf JFM, Boersema JR, Van Gelder A (1977) Waves-generated structures and sequences from a  
14 shallow marine section, lower Carboniferous, Country Cork, Ireland. *Sedimentology* 24: 451- 483
- 15 Dewey JF, Helman ML, Knott SD, Hutton DHW (1989) Kinematics of the western Mediterranean.  
16 *Geological Society London Special Publications* 45 (1): 265-283
- 17 Dickinson WR, Rich EI (1972) Petrologic intervals and petrofacies in the Great Valley Sequence,  
18 Sacramento Valley, California: *Geol. Soc. America Bull* 83: 3007–3024
- 19 Durand-Delga M, Hottinger L, Marcáis J, Mattauer M, Milliard Y, Suter G (1962) Données nouvelles sur la  
20 structure du Rif. *Mém. h. sér. Soc. géol., France* 399- 422
- 21 Frey RW, Howard J D, Pryor WA (1978) Ophiomorpha: its morphologic, taxonomic, and environmental  
22 significance. *Palaeogeogr., Palaeoclimatol., Palaeoecol.* 23: 199- 229.
- 23 Fürsich F, Taheri J, Wilmsen M (2007) New occurrences of the trace fossil *Paleodictyon* in shallow marine  
24 environments: Examples from the Triassic-Jurassic of Iran. *Palaios.* 22: 408-416.
- 25 Galloway WE (1975) Process framework for describing the morphologic and stratigraphic evolution of  
26 deltaic depositional systems. In: Broussard ML (ed) *Deltas: models for exploration*. Houston Geological Society,  
27 Houston, 87–98
- 28 Guiraud R, Bosworth W, Thierry J, Delaplanque A. (2005) Phanerozoic geological evolution of northern  
29 and central Africa: an overview. *Journal of African Earth Sciences* 43, 83–143.

1 Goodbred S L jr, Saito Y (2012) Tide-Dominated Deltas. R.A. Davis, Jr. and R.W. Dalrymple (eds.),  
2 Principles of Tidal Sedimentology, 129, Springer Science.

3 Hamoumi N (1995a) Réinterprétation des contacts situés entre les unités des flyschs du Déroit de Gibraltar  
4 et de sa rive sud -Intérêt des études sédimentologiques et géophysiques pour le Projet Liaison Fixe Europe-  
5 Afrique. Actes du IV Coloquio Internacional sobre el Enlace Fijo Estrecho de Gibraltar, Tomo II El Medio  
6 Fisico, SNED & SECEG Edit., pp. 217- 224

7 Hamoumi N, Salhi F, Ouldchalha A (1995a) L'Oligo-Miocène de la rive sud du Déroit de Gibraltar (Rif-  
8 Maroc) : Faciès et environnements sédimentaires, contrôle géodynamique et eustatique. Actes du IV Coloquio  
9 Internacional sobre el Enlace Fijo Estrecho de Gibraltar, Tomo II El Medio Fisico, SNED & SECEG Edit., pp.  
10 21- 50

11 Hamoumi N (1995b) Les ensembles géologiques de subsurface dans la région du Puits Malabata : Etude  
12 sédimentologique et géochimique- Essai de corrélation Actes du IV Coloquio Internacional sobre el Enlace Fijo  
13 Estrecho de Gibraltar, Tomo II El Medio Fisico, SNED & SECEG Edit., pp. 225- 247

14 Haq BU, Hardenbol J, Vail PR (1987) Chronology of fluctuating sea levels since the Triassic (250 million  
15 years ago to present). Science 235: 1156–1166.

16 Harms JC, Southard JB, Spearing DR, Walker RG (1975) Depositional environments as interpreted from  
17 primary sedimentary structures and stratification sequences. Soc. Econ. Paleont. Mineral., Short Course 2, Dallas

18 Howard JD, Reineck HE (1981) Depositional Facies of High-Energy Beach-to-Offshore Sequence:  
19 Comparison with Low-Energy Sequence. American Association of Petroleum Geologists Bulletin, 65: 807-830

20 Jelby ME, Grundvåg SA, Helland-Hansen W, Olaussen S, Stemmerik Lars (2019) Tempestite facies  
21 variability and storm-depositional processes across a wide ramp: Towards a polygenetic model for hummocky  
22 cross-stratification. Sedimentology: 10.1111.

23 Knaust D (2004) Cambro-Ordovician trace fossils from the SW Norwegian Caledonides. Geological  
24 Journal. 39: 1 – 24.

25 Kreisa RD, Moiola RJ (1986) Sigmoidal tidal bundles and other tide-generated sedimentary structures of  
26 the Curtis Formation. Geological Society of America Bulletin (97) 4: 381-387

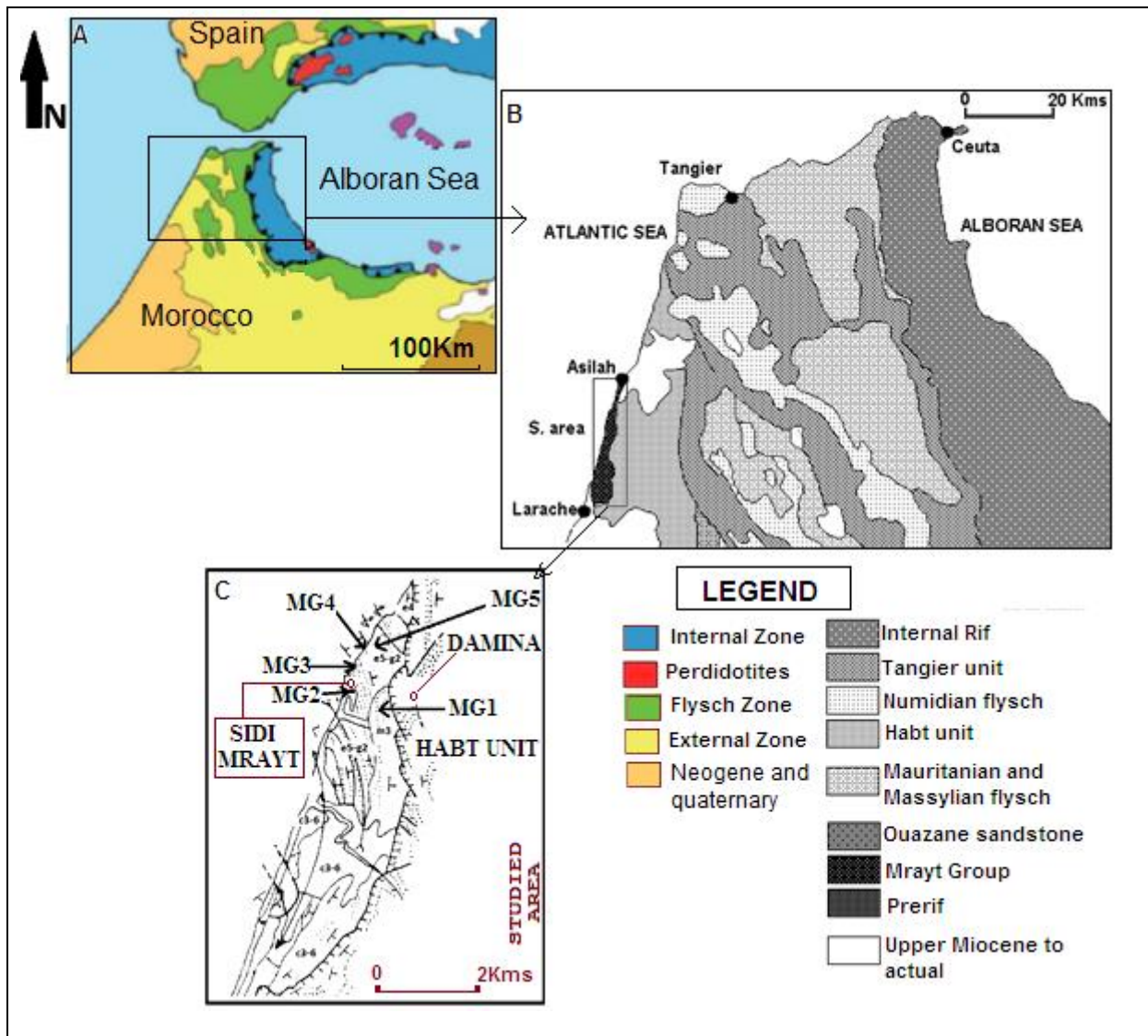
- 1           Leprêtre R, Frizon de Lamotte D, Combier V, Gimeno-Vives O, Mohn G, Eschard R (2018) The Tell-Rif  
2 orogenic system (Morocco, Algeria, Tunisia) and the structural heritage of the southern Tethys margin. BSGF -  
3 Earth Sciences Bulletin, 189, 10.
- 4           Lowe DR (1975) Water escape structures in coarse grained sediments. *Sedimentology*, 22: 157-204
- 5           Mansfield GR (1971) Origin of the Brown Mountain light in North Carolina, Geological Survey (U.S.): 18,  
6 647
- 7           Metz R (2012) The Trace Fossil *Paleodictyon* within The Cruziana Ichnofacies: First Record from The  
8 Devonian in Pennsylvania. *Ichnos* 19: 10.1080
- 9           Mowbray T, Visser M (1984) Reactivation surfaces in subtidal channel deposits, Oosterschelde, Southwest  
10 Netherlands. *Journal of Sedimentary Petrology*, 54 (3): 811–824
- 11          Mutti E (1985) Turbidite Systems and Their Relations to Depositional Sequences. In Zuffa G. G. ed.  
12 Provenance of arenites Dordrecht, D. Reidel Publishing Company, 65–93
- 13          Miall A D (1992) Alluvial deposits Facies models, response to sea level change. In: Walker RG, James N  
14 P, (eds). *Facies Models: Response to Sea Level Change*. Geological Association of Canada, St. John's, 119-142
- 15          Morley CK (1992) Tectonic and sedimentary evidence for synchronous and out-of-sequence thrusting,  
16 Larache-Acilah area, western Moroccan Rif. *J. Geol. Soc., London*, 149: 39- 49
- 17          Mount JF (1985) Mixed siliciclastic and carbonate sediments: a proposed first-order textural and  
18 compositional classification. *Sedimentology*, 32: 435-442
- 19          Nesbitt E A, Campbell K A (2006) The Paleoenvironmental Significance of *Psilonichnus*. *PALAIOS* 21  
20 (2): 187–196.
- 21          Nio SD, Yang CS (1989) Recognition of tidally-influenced Facies and Environments. *International*  
22 *Geoservices BV*, 230
- 23          Ouldchalha A, Hamoumi N, Salhi F (1995) Les flyschs d'âge éocène de la Rive sud du Détroit de Gibraltar  
24 (Rif, Maroc) : Faciès et environnements sédimentaires, contrôle géodynamique et eustatique. *Actes du IV*  
25 *Coloquio Internacional sobre el Enlace Fijo Estrecho de Gibraltar, Tomo II El Medio Físico, SNED & SECEG*  
26 *Edit., pp. 339- 350*
- 27          Odin G S (1985) Significance of green particles (glaucony, berthierine, chlorite) in arenites. In *Provenance*  
28 *of arenites, GG Zuffa (Ed.), NATO ASI Series, V 148:279-307*

- 1 Pandey DK, Uchman A, Kumar V, Shekhawat RS (2014) Cambrian trace fossils of the Cruziana  
2 ichnofacies from the Bikaner-Nagaur Basin, north western Indian Craton. *Journal of Asian Earth Sciences*, 81:  
3 129–141
- 4 Pettijhon FJ, Potter PE, Siever R (1973) *Sand and Sandstone* pp. 617, Springer-Verlag, Berlin
- 5 Platt JP, Vissers RLM (1989) Extensional collapse of thickened continental lithosphere: A working  
6 hypothesis for the Alboran Sea and Gibraltar arc. *Geology* 17, 540-543
- 7 Raissouni A, Raibi F, Tejera De Leon J, Dakki M (2008) Les Grès de Mrayt : un environnement de  
8 plateforme externe soumis à l'action des houles de tempête. Evolution de l'Eocène au Miocène moyen (Rif Nord  
9 occidental). 20ème Colloque Bassins sédimentaires Marocains, Oujda
- 10 Reading HG (1986) *Sedimentary Environments and Facies*. Blackwell Scientific Publications, Oxford, 471-  
11 519
- 12 Reineck H E (1969) Die Entstehung von Runzelmarken. *Nat. Mus.* 99: 386-388
- 13 Reineck HE, Singh IB (1980) *Depositional Sedimentary Environments*, Springer-Verlag, Berlin,  
14 Heidelberg, New York
- 15 Salhi F, Hamoumi N, Oueddhalha A (1995) Les flyschs d'âge crétacé de la rive sud du Déroit de Gibraltar  
16 (Rif-Maroc): Faciès et environnements sédimentaires, contrôle géodynamique et eustatique. Actes du IV  
17 Coloquio Internacional sobre el Enlace Fijo Estrecho de Gibraltar, Tomo II El Medio Fisico (SNED & SECEG  
18 Edit.), pp. 361- 375
- 19 Shahin D, Murray G, Maceachern J (2009) Tidally Modulated Shorefaces. *Journal of Sedimentary  
20 Research*. 79: 793-807
- 21 Seilacher A (1967) Bathymetry of trace fossils. *Marine Geology*, 5: 4, 13- 42
- 22 Srivastava S, Schouten H., Roest W, Klitgord K., Kovacs L., Verhoef J, Macnab R (1990) Iberian Plate  
23 kinematics: a jumping plate boundary between Eurasia and Africa. *Nature*
- 24 Suter G, Fiechter G (1966) Le Rif méridional atlantique (Maroc) : aperçu structural sur la région Ouezzane-  
25 Zoumi et le pays du Habt (Larache). *Notes Mém. Serv. Géol. Maroc* (26) 188: 15-20
- 26 Suter G (1980) Carte géologique de la chaîne rifaine au 1/50 000. *Notes Mém. Serv. Géol. Maroc* 245a & b
- 27 Suter G (1986) Carte géologique de la chaîne rifaine au 1/50 000. *Notes Mém. Serv. Géol. Maroc* 346
- 28 Swezey CS (2009) Cenozoic stratigraphy of the Sahara, Northern Africa. *Journal of African Earth  
29 Sciences* 53 89–121

- 1 Swift DJP, Figueiredo Jr, Freeland G, Oertel GF (1983) Hummocky Cross-Stratification and Megaripples:  
2 A Geological Double Standard? *Journal of Sedimentary Petrology*, 53 :1295-1317
- 3 Tejera de Leon J (1993) Les bassins néogènes d'avant-pays du Rif externe occidental liés à la  
4 transformante Jebha-Arbaoua (Maroc).Thèse Doct. Etat. es Sciences, Univ. de Pau et des Pays de l'Adour 323 p.
- 5 Terwindt JHJ (1981) Origin and sequences of sedimentary structures in mesotidal deposits of the North  
6 Sea. *Spec. Publ. Int. Assoc. Sedimentol.*5: 4–26
- 7 Tessier B, Monfort Y, Gigot P, Larsonneur C (1989) Enregistrement des cycles tidaux en accréation  
8 verticale, adaptation d'un outil de traitement mathématique. Exemples en baie du Mont-Saint-Michel et dans la  
9 molasse marine miocene du bassin de Digne. *Bull. Soc. Géol. Fr.* 8: 1029-1041
- 10 Visser MJ (1980) Neap-spring cycles reflected in Holocene subtidal large-scale bedform deposits. A  
11 preliminary note. *Geology*, 8: 543-546
- 12 Wildi W (1983) La chaîne tello-rifaine: Structure, Stratigraphie et évolution du Trias au Miocène. *Revue de*  
13 *Géologie dynamique et de Géographie Physique*, 24, 201-297
- 14 Wright LD, Short AD (1984) Morphodynamic variability of surf zones and beaches: A synthesis, *Marine*  
15 *Geology*, 56: Issues 1–4, 93-118
- 16 Wright LD, Friedrichs C (2006) Gravity-driven sediment transport on continental shelves: A status report,  
17 *Continental Shelf Research - CONT SHELF RES*, 26: 2092-2107
- 18 Yang BC, Dalrymple R, Chun SS (2006) The Significance of Hummocky Cross-Stratification (HCS)  
19 Wavelengths: Evidence from an Open-Coast Tidal Flat, South Korea. *Journal of Sedimentary Research*, 76: 2-8.
- 20 Zachos JM, Pagani L, Sloan E, Thomas K., Billups K (2001) Trends, Rhythms, and Aberrations in Global  
21 Climate 65 Ma to Present.*Science*, 292, Issue 5517, 686-693.
- 22 Zhang LJ, Zhao Z (2016) Complex behavioural patterns and ethological analysis of the trace fossil  
23 *Zoophycos*: evidence from the Lower Devonian of South China. *Lethaia* 49:275–284.

24  
25  
26  
27  
28  
29

1 Fig. 1



2

3 A geological map of the geological domains in the Betic-Rif orogenic system (after Platt and Vissers 1989); B Location of

4 the Mrayt Group outcrops in the geological map of the North Western Rif (after Suter 1980); C Location of the studied

5 outcrops in the structural map of Suter (1980): MG1- Damina section, 80m thick (X= 6.06; Y= 35.42), MG2- Marabout

6 section, 750m thick (X= 5.85; Y= 35.36), MG3- Sidi Mrayt beach section, 200m thick (X= 5.85; Y= 35.41), MG4- Merja

7 section, 520m thick (X= 5.96; Y= 35.43), and MG5- Merja ravine section, 280m thick (X= 6.05; Y= 35.44). S. area: Studied

8 area

9

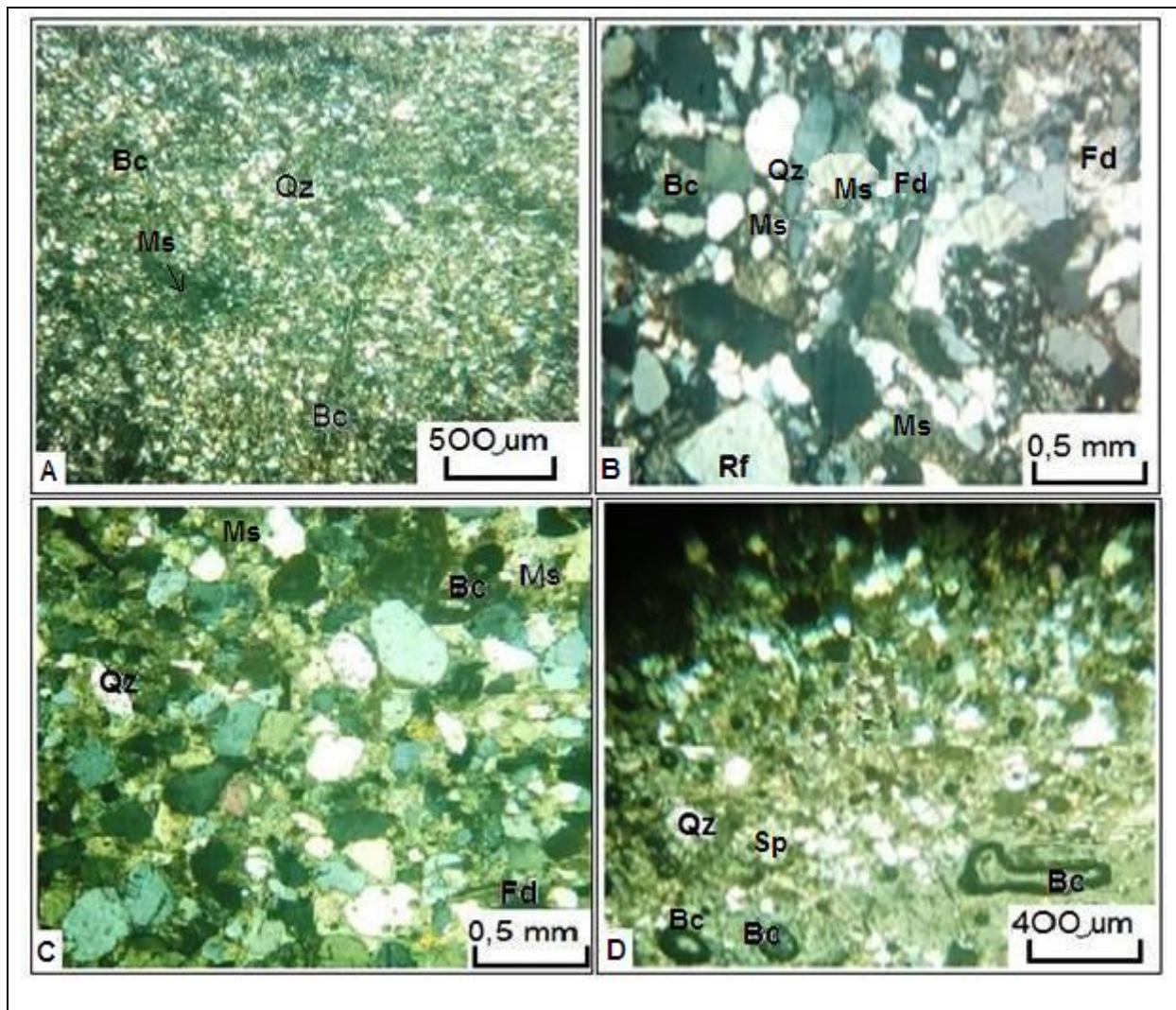
10

11

12

13

1 **Fig. 2**



2

3 Petrofacies of the Mrayt Group: A- micritic siltstone; B- sandy micrite; C- micritic sandstone; D- sandy allochemic sandstone. Bc-

4 Bioclasts, Qz- Quartz, Sp- Sparite, Ms- microsparite, Fd- fedspath, Rf- Rock fragment

5

6

7

8

9

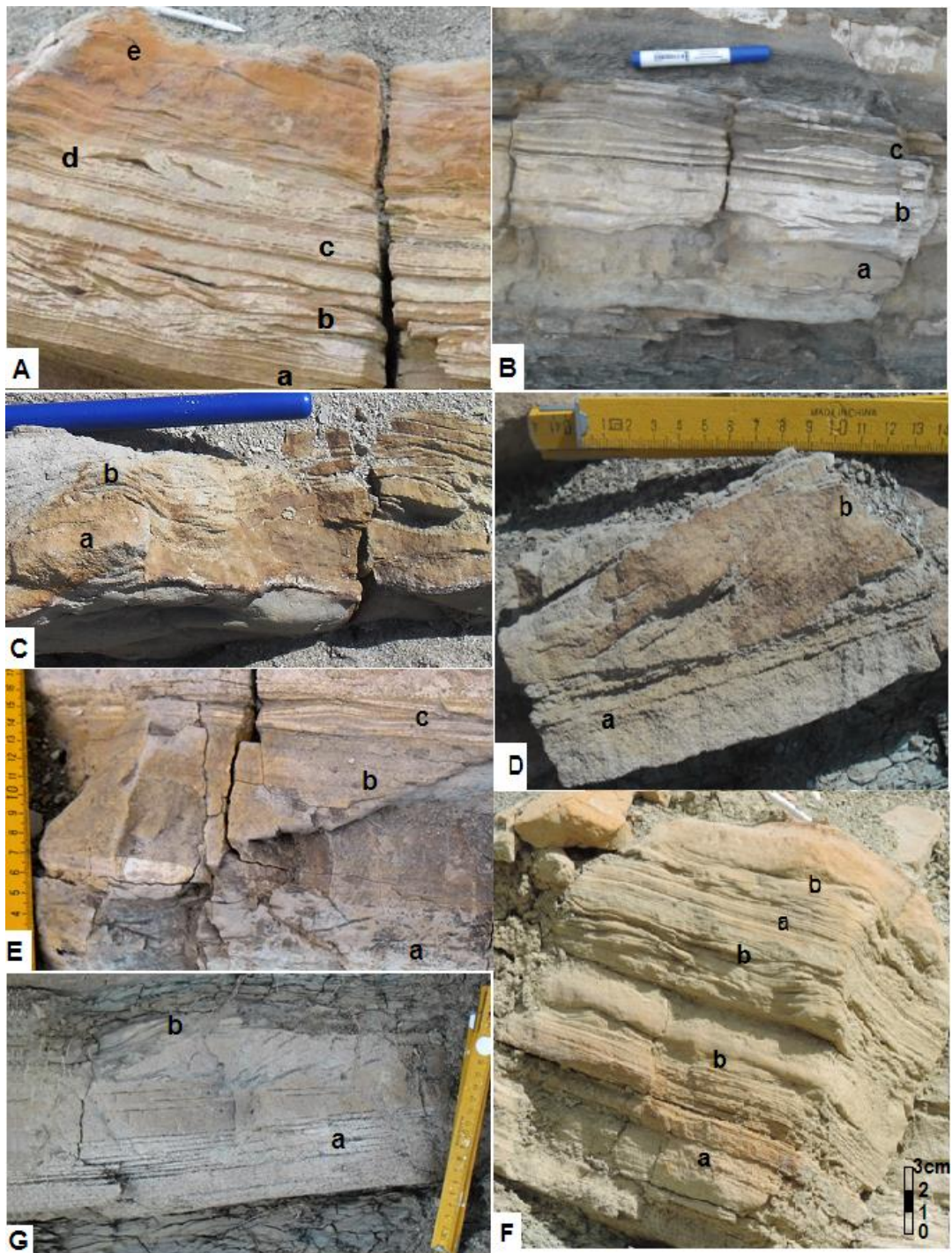
10

11

12

13

1 **Fig. 3**

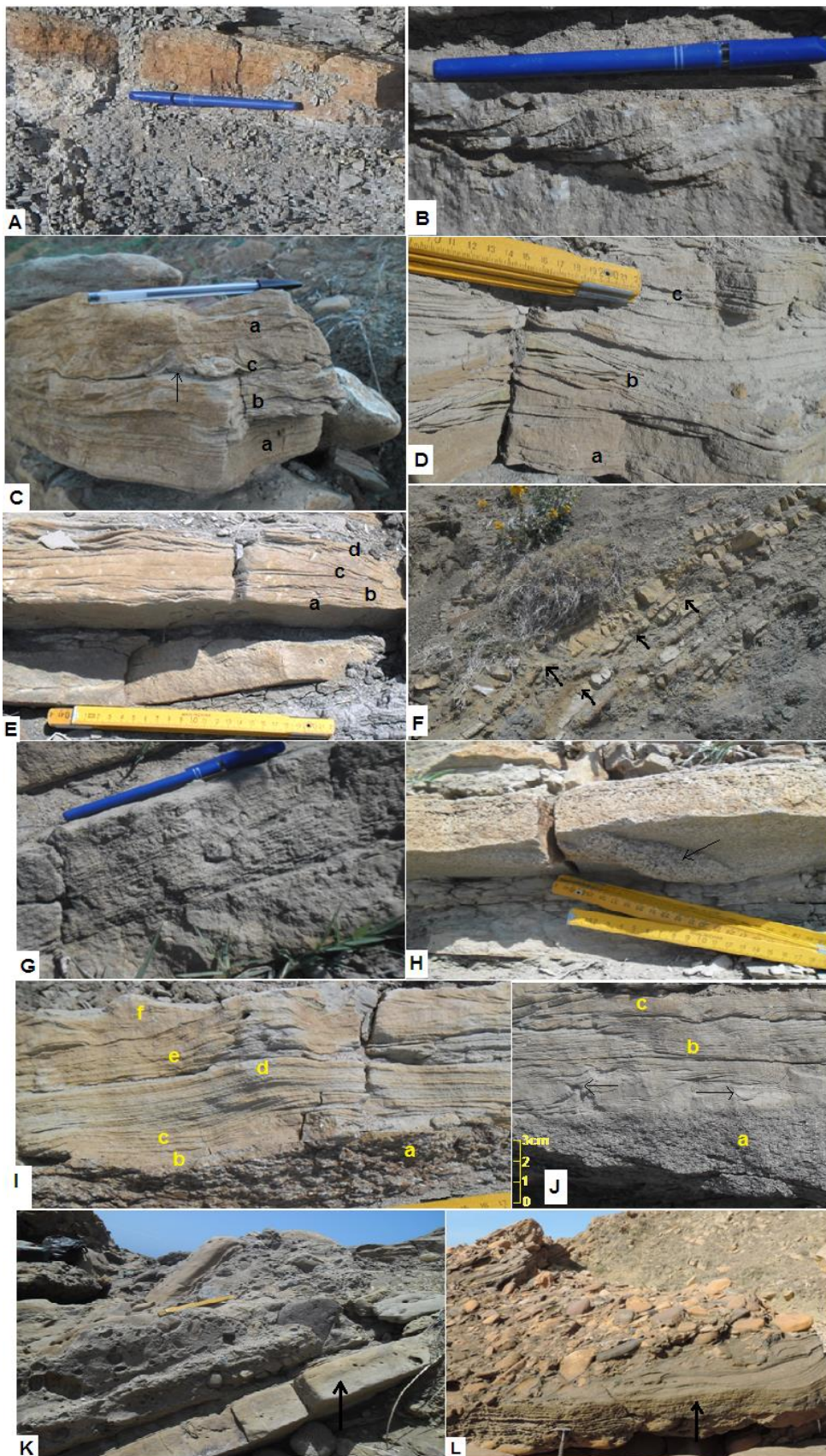


2

3 Sedimentary facies. A- Facies F1 (a and c- mud couplets, b-flaser bedding, d- wavy bedding, e-lenticular bedding). B- Facies F2  
 4 (a and c- mud couplets, b-flaser bedding, c- asymmetrical ripples); C- Facies F3 (a- slightly deformed level without visible  
 5 bedding, b- asymmetrical ripples); D- Facies F4 (a- parallel undulated plane laminations, b- tangential oblique laminations); E-  
 6 Facies F5 (a- mud pebbles, b- massive level, c- parallel undulated lamination); F- Facies F6 (a- rhythmic parallel laminations, b-  
 7 tidal bundles); G- Facies F7 (a- tidal rhythmites, b- tidal bundles)

8





1     **Fig.4** Sedimentary facies. A- Facies F8; B- Facies F9; C- Facies F10 (a- mud couplets, b- sigmoidal bundles, c- symmetrical  
2 ripples, arrows indicate flame structures); D- Facies F11 (a- tidal bindles, b-cross laminated beds, c- tidal rhythmites; E- Facies  
3 F12 (a- asymmetrical ripples, b- tidal rhythmites, c- cross laminated beds , d- tidal bundles); F- Facies F13 (arrows indicate  
4 hummocks); G- detail of F13: Hummocky cross stratification; H- Facies F14 (arrows indicate flute cast); I- Facies F15 (a-  
5 microconglomerate, b- massive level, c- asymmetrical ripples, d- tidal rhythmites, e- tidal bundles, f- asymmetrical ripples); J-  
6 Facies F16 (a- microconglomerate, b- tidal rhythmites, c- tidal bundles, arrow indicate convolute bedding); K- Facies F17 a and b  
7 (arrow indicate medium to fine -grained sandstone bed); L- Facies F17c (arrow indicate coarse sandstone bed)

8

9

10

11

12

13

14

15

16

17

18

19

20

21

22

23

24

25

26

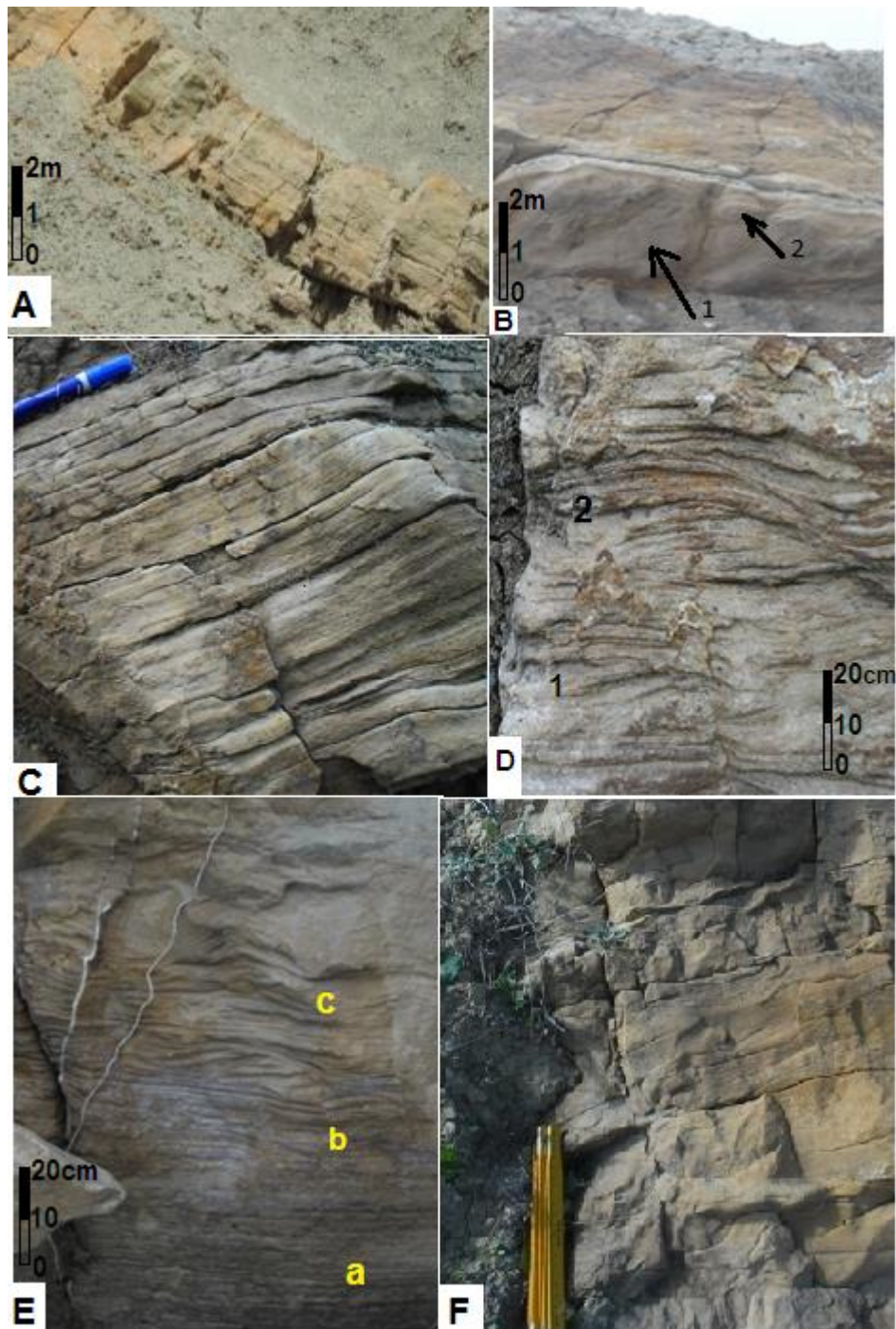
27

28

29

30

1 Fig. 5

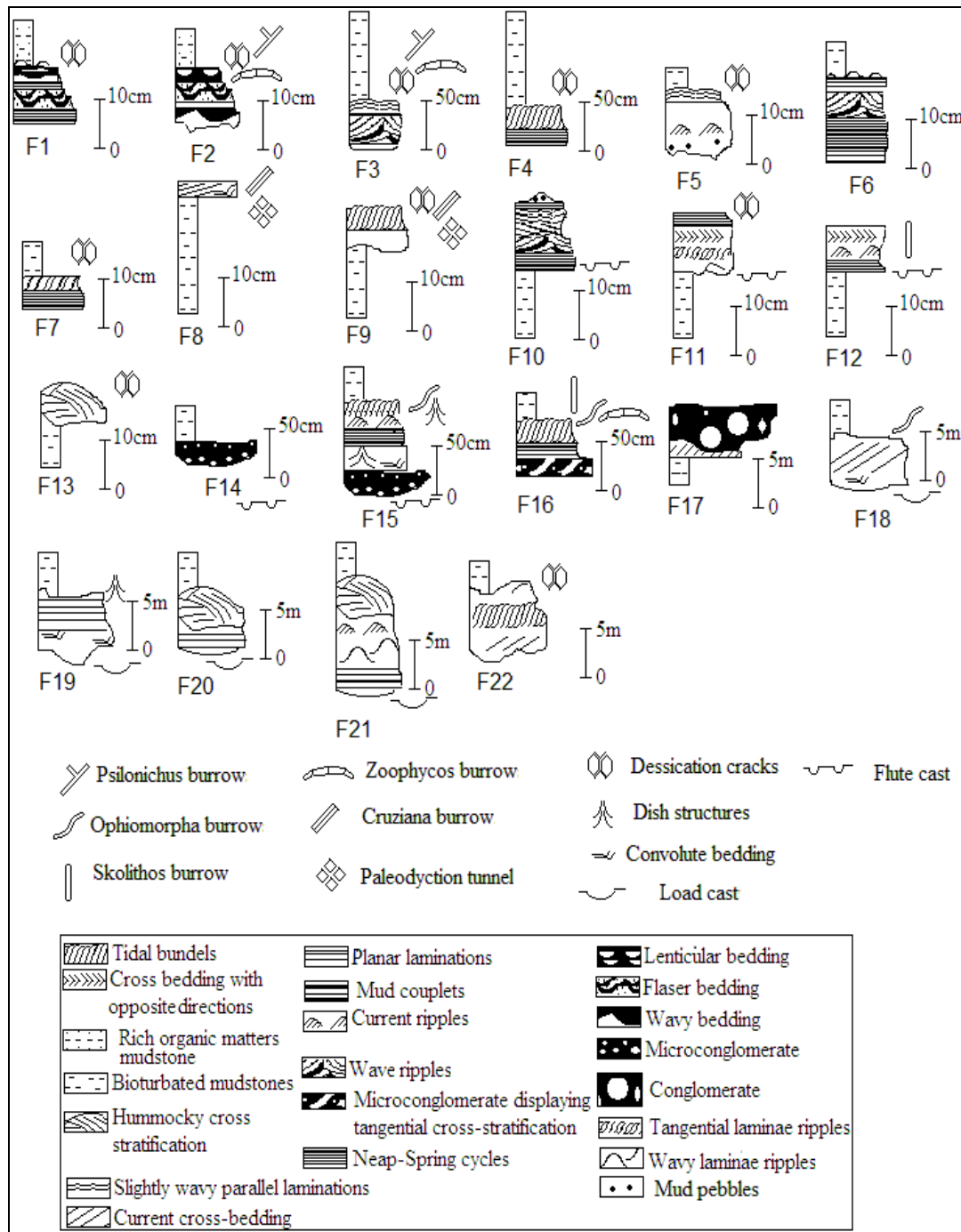


2

3 Sedimentary facies. A- Low-angle cross lamination in Facies F18; B- Load casts (arrows 1: large-scale and 2: small-scale) at  
4 the base of Facies F18; C- Facies F19; D- Facies F20 (1- planar parallel lamina and 2- Hummocky cross stratification); E-  
5 Facies F21 (a- tidal rhythmites, b- symmetrical wave ripples passing to megaripple cross bedding, c- micro-hummocky cross  
6 stratification); E- Facies F21 (a- tidal rhythmites, b- symmetrical wave ripples passing to megaripple cross bedding, c- micro-  
7 hummocky cross stratification); F- Facies F22

8

1 **Fig. 6**



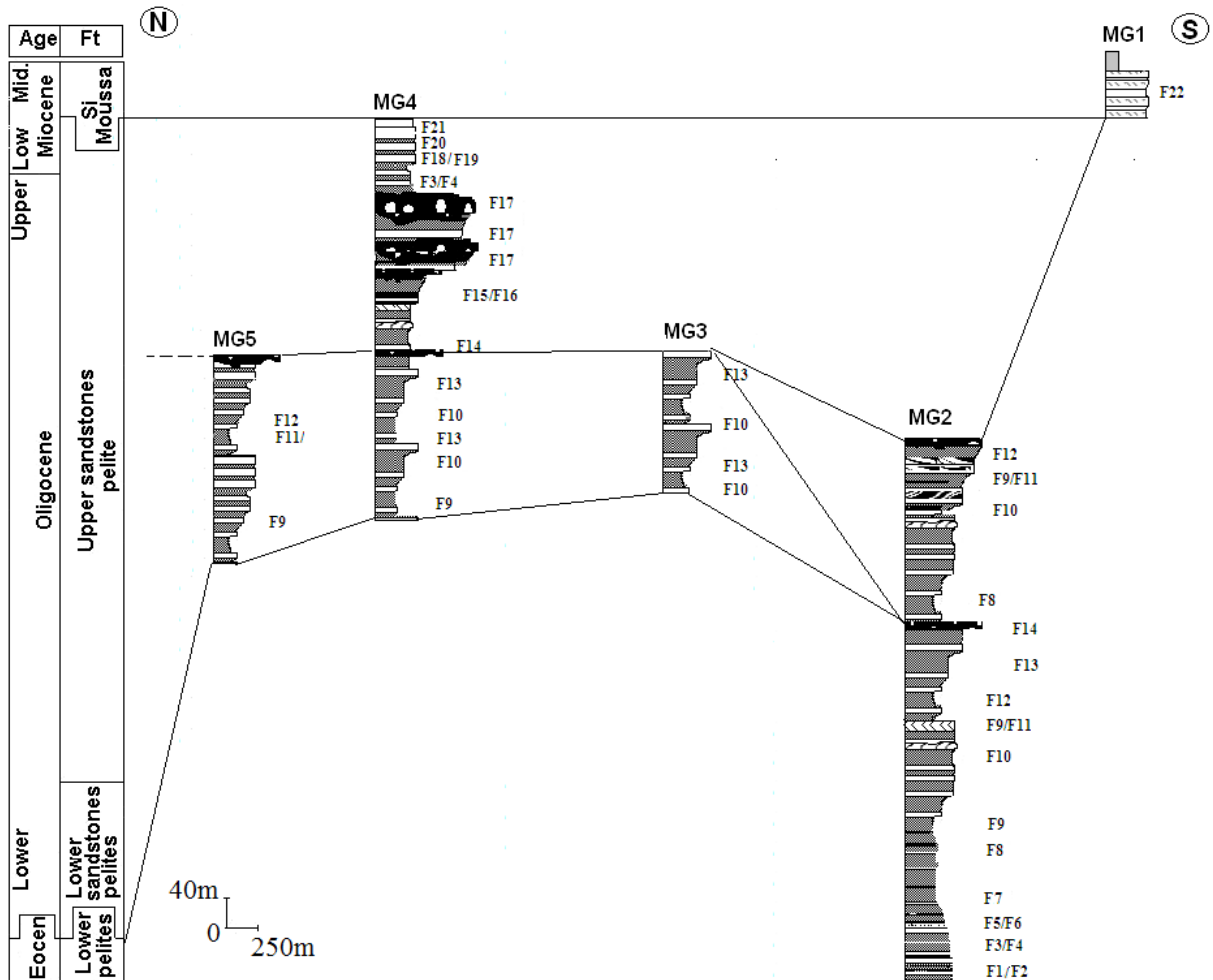
2  
3 **Facies of the Mrayt Group**

4

5

6

1 Fig. 7



2

3 Studied outcrops from the Mrayt Group: MG1- Damina section, MG2- Marabout section, MG3- Sidi Mrayt beach section, MG4-

4 Merja section, and MG5- Merja ravine section (See locations and thick in Fig.1C)

5

6

7

8

9

10

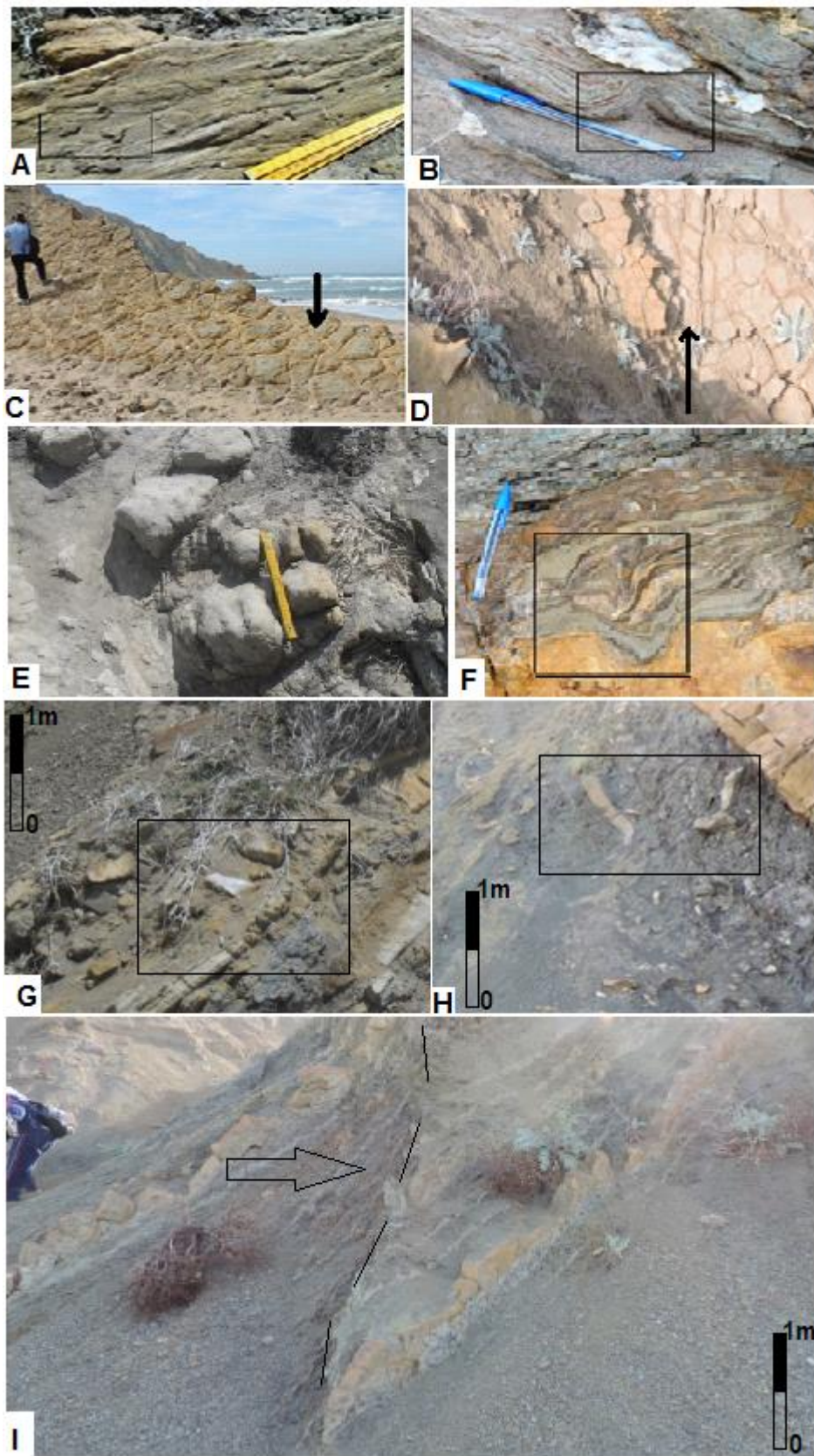
11

12

13

14

1 Fig. 8

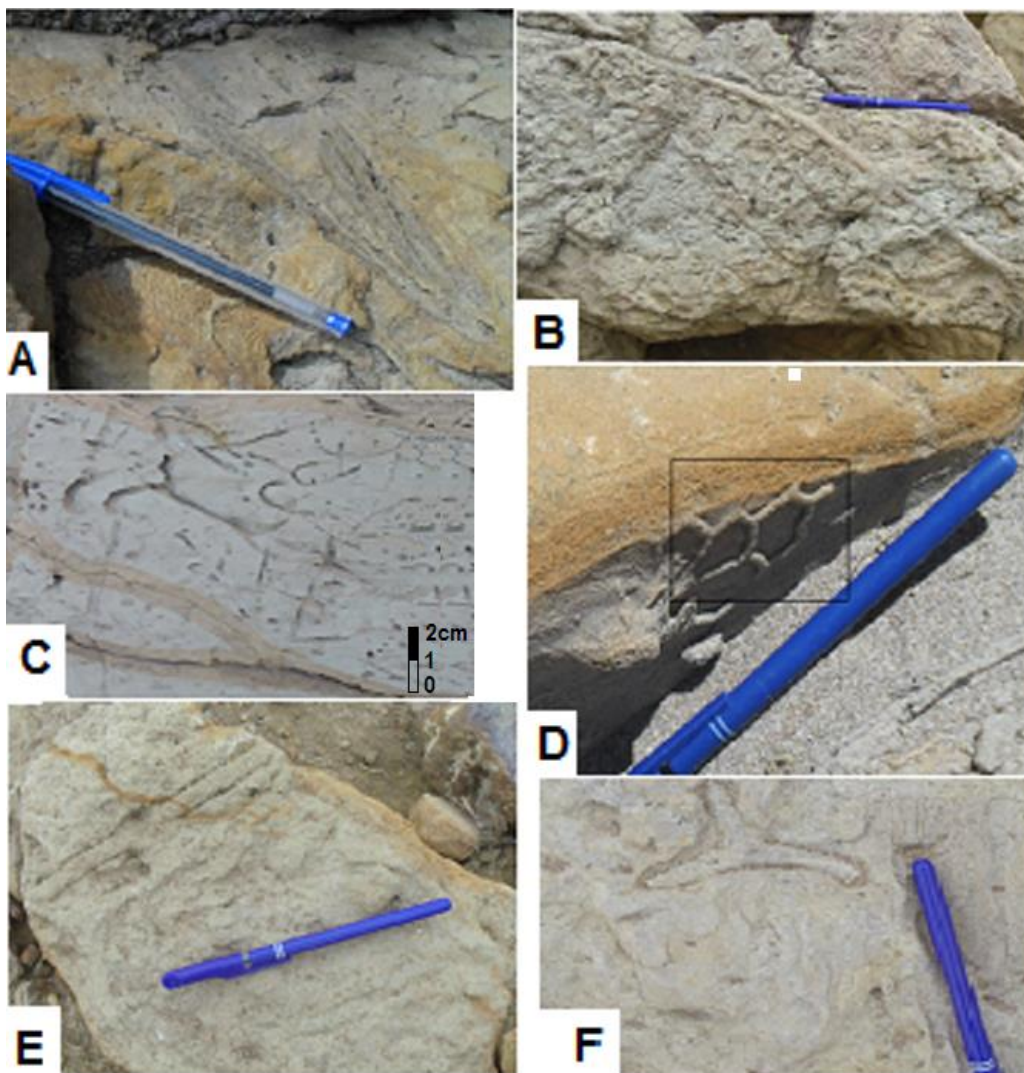


2

1 Sedimentary structures. A- Flute casts (F10, observed also in F1, F11, F12, F14 and F15); B- dish and pillar structures (F15,  
2 observed also in F19); C- large scale desiccation cracks observed in F3 in the upper pelites formation; D- cm to dm desiccation  
3 cracks (F11, observed also in F1, F2, F3, F4, F5 F7, F9, F13 and F22); E-ball and pillow (F16, observed also in F20); F-  
4 convolutes bedding (F15, observed also in F8, F16, F18, and F19); G-synsedimentary deformations in the lower pelites  
5 formation; H- synsedimentary deformations in the lower sandstones formation; I- synsedimentary deformations in the upper  
6 pelites formation (dashes show synsedimentary tectonics)

7

8 **Fig. 9**

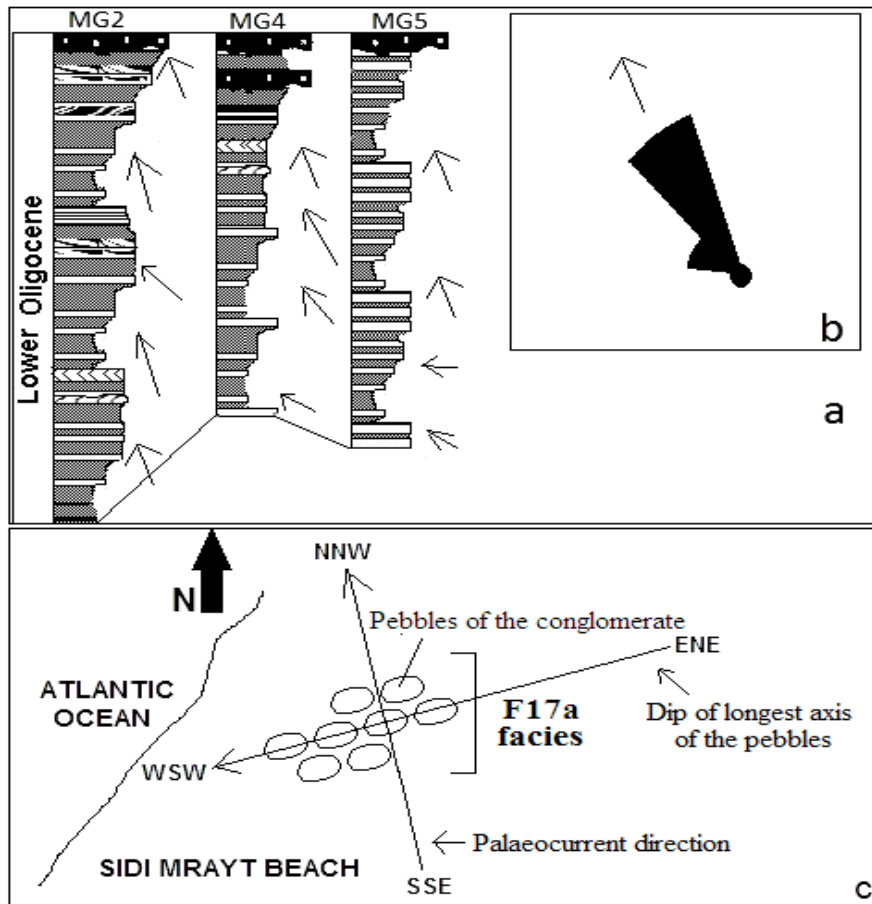


9

10 Trace fossils. A- Zoophycos burrow (F12); B- Ophiomorpha burrow (F10, observed also in F12, F13 and F16); C- Skolithos  
11 burrow (F12, observed also in F13); D- Palaeodictyon tunnel (F4); E- Cruziana burrow; F- Psilochinus burrow

12

1 **Fig. 10**



2

3 Palaeocurrent measurements (a) and the rose diagram (b) (main direction SSE to NNE, n=48). MG2- Marabout delta, MG4-

4 Merja delta, and MG5- Merja ravine delta (locations in Fig.1C), dip of longest axis of pebbles (c)

5

6

7

8

9

10

11

12

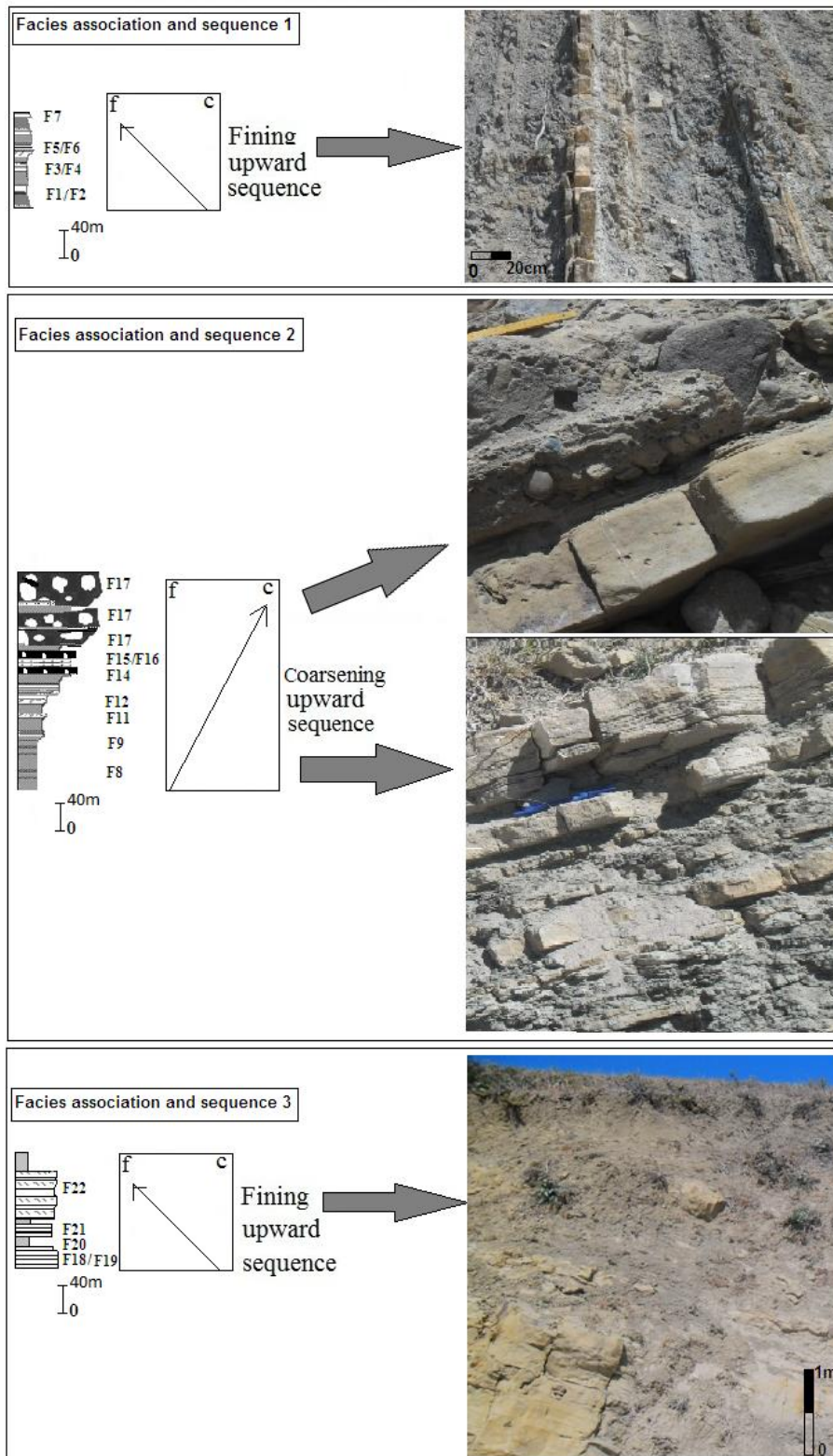
13

14

15



1 Fig. 11

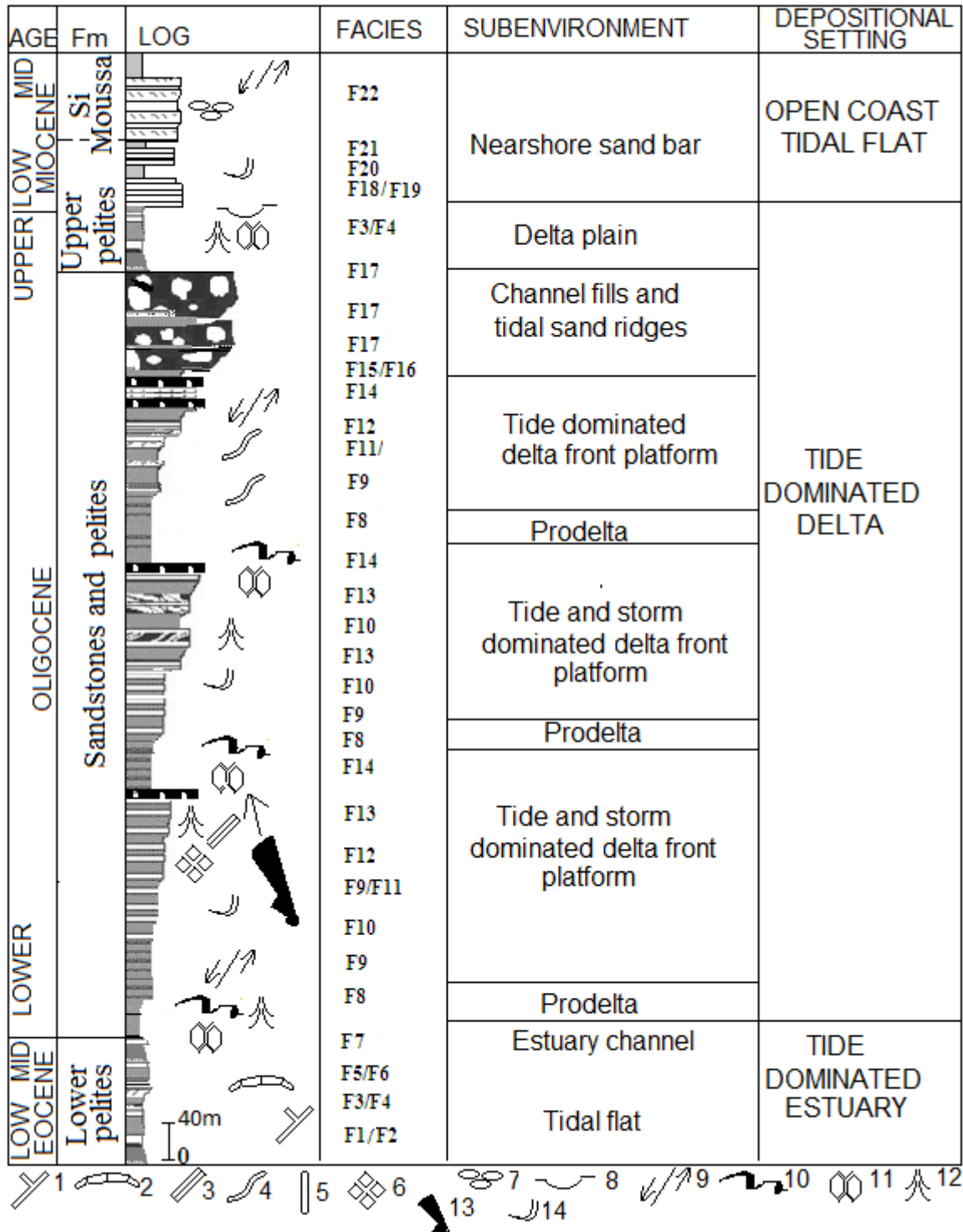


2

3 Facies associations and sequences of the Mrayt Group. f: fine grained sediment. c: coarse grained sediment

4

1 Fig. 12



2

3 Lithology, sedimentary environments and depositional sequences of Mrayt Group (1- Ppsilonichus burrows, 2-Zoophycos  
 4 burrows, 3- Cruziana burrows, 4- ophiomorpha burrows, 5- skolithos burrows, 6- Paleodictyon tunnels, 7- ball and pillow, 8- load  
 5 cast, 9- syndimentary fault, 10- convolute bedding, 11- dessication cracks, 12- dish and pillar structure, 13- palaeocurrent  
 6 measurements), 14- slumps, Fm: Formation